Atomic Scale Processing Focus Topic
Room A214 - Session AP+2D+EM+PS+TF-MoM

Area Selective Deposition and Selective-Area Patterning

Moderators: Satoshi Hamaguchi, Osaka University, Japan, Eric A. Joseph, IBM T.J. Watson Research Center

8:40am **AP+2D+EM+PS+TF-MoM2 Surface Pre-functionalization of SiN_x and SiO_2 to Enhance Selectivity in Plasma–Assisted Atomic Layer Etching***, **Ryan Gasvoda**, Colorado School of Mines; Z. Zhang, S. Wang, E.A. Hudson,* Lam Research Corporation*; S. Agarwal,* Colorado School of Mines

To manufacture semiconductor devices in the current sub-7-nm node, stringent processing windows are placed on all aspects in manufacturing including plasma-etching. In recent years, atomic layer etching (ALE) has emerged as a patterning technique that can provide high etch fidelity, directionality, layer–by–layer removal, and selectivity to meet the tight processing windows. Plasma–assisted ALE of SiO_2 and SiN_x is of particular interest since Si-based dielectrics are commonly used throughout the entire fabrication process. Typically, these materials are etched in a cyclic ALE process consisting of two sequential half–cycles: fluorocarbon (CF_x) deposition from a fluorocarbon plasma followed by an Ar plasma activation step. Etch selectivity can be achieved through careful manipulation of the plasma and processing parameters. To further increase overall etch selectivity, we have proposed a methodology that selectively pre–functionalizes the SiO_2 or SiN_x surface with hydrocarbons prior to ALE. Recently, we showed that an etch blocking graphitic hydrofluorocarbon film will readily accumulate on a pre–functionalized SiO_2 surface.

In this study, we used *in situ* attenuated total reflection Fourier transform infrared (ATR–FTIR) spectroscopy and *in situ* 4–wavelength ellipsometry to monitor the surface reactions, film composition, and net film thickness during the entire ALE process. We show that aldehydes can be used to functionalize SiN_x with extremely high selectivity to SiO_2 surfaces. During ALE on bare SiN_x, a thick graphitic fluorocarbon film accumulates on the surface and can stop all etching after cycle 5. This is attributed to inefficient removal of both the C and N from the surface. To enhance removal and prevent graphitic carbon accumulation, we graft a branched hydrocarbon aldehyde to the SiN_x surface. This branched hydrocarbon provides an abundance of $–CH_3$ groups which allows for greater C and N removal possibly via HCN formation, thus lowering overall graphitic carbon formation. This retardation of the graphitic hydrofluorocarbon film formation leads to both an overall increase in the etch per cycle and the number of ALE cycles that can be run before an etch stop is observed.

9:00am **AP+2D+EM+PS+TF-MoM3 Area-selective Atmospheric-pressure Spatial ALD of SiO_2 using Interleaved Back-etch steps Yielding Selectivity > 10 nm***, A. Mameli,* Holst Centre / TNO, The Netherlands*; F. Roozeboom,* ***Paul Poodt****,* Holst Centre / TNO, The Netherlands, Netherlands

Area-selective atomic layer deposition (AS-ALD) has great potential in reducing cost by maskless device manufacturing of patterned layers. Still, in this new *bottom-up* approach the selectivities currently obtained for film growth on patterned growth areas vs. that on the non-growth areas are often very limited. Also the substrate throughput values for conventional low-pressure ALD is too low for industrial acceptance.(1,2) In this work we present a process for AS-ALD of SiO_2 using intermittent plasma etch-back steps to increase the selectivity above 10 nm film thickness.(3) In addition, the deposition process itself is performed in a spatial ALD reactor at atmospheric pressure which allows for achieving high throughput.(4)

AS-ALD of SiO_2 on a substrate with pre-patterned SiO_2 and ZnO areas was demonstrated using a highly chemo-selective inhibitor that chemisorbs preferentially on the non-growth area (ZnO) while allowing the deposition of SiO_2 on the growth area (SiO_2). In order to maximize the process selectivity, a blanket fluorocarbon plasma etch-back step was interleaved after every 110 ALD cycles. This way, selective SiO_2 deposition up to ~ 30 nm film thickness was demonstrated. Furthermore, X-ray Photoelectron Spectroscopy was carried out to verify the selectivity of the process: no Si was detected (detection limit 0.3 at. %) on the non-growth area, demonstrating the high selectivity of the process.

The process presented here combines selective inhibitor chemisorption, plasma-based spatial ALD with high deposition rates and plasma etch-back steps to correct for selectivity loss. This approach is compatible with *roll-to-roll* and *sheet-to-sheet* concepts and can therefore enable high-throughput AS-ALD on large-area and flexible substrates.

[1] A. Mameli, *et al.*, *ACS Nano*, **11**, 9303 (2017).

[2] F.S.M. Hashemi, *et al.*, *ACS Nano*, **9**, 8710 (2015).

[3] R. Vallat, *et al.*, *J. Vac Sc. Technol. A*, **35**, 01B104 (2017).

[4] P. Poodt, *et al.*, *Adv. Mater.*, **22**, 3564 (2010).

9:20am **AP+2D+EM+PS+TF-MoM4 Mechanisms of Precursor Blocking during Area-selective Atomic Layer Deposition using Inhibitors in ABC-type Cycles***, M.J.M. Merkx,* Eindhoven University of Technology, The Netherlands*; D.M. Hausmann,* Lam Research Corporation*; W.M.M. Kessels,* Eindhoven University of Technology, The Netherlands, Netherlands*; T.E. Sandoval,* Universidad Técnica Federico Santa María, Chile*;* ***Adrie Mackus***[1]*,* Eindhoven University of Technology, The Netherlands, Nederland

The development of new processes for area-selective atomic layer deposition (ALD) is currently motivated by the need for self-aligned fabrication schemes in semiconductor processing. For example, area-selective ALD processes for dielectric-on-dielectric deposition are being considered for fully self-aligned via (FSAV) fabrication schemes in advanced interconnect technology.

Instead of solely relying on surface functionalization prior to ALD, an novel strategy to area-selective ALD involves the dosing of inhibitor molecules during every cycle in an ABC-type recipe.[1,2] By using small molecules that can be dosed in vapor-phase as inhibitor, this approach is compatible with industrial process flows. Moreover, the reapplication of the inhibitor molecules during every cycle allows for the use of a plasma as the co-reactant, which broadens the range of materials that can be deposited selectively. In contrast to conventional approaches to area-selective ALD based on self-assembled monolayers (SAMs), very little is known about how small inhibitor molecules can block the ALD growth.

In this contribution, insight into the mechanisms of precursor blocking by inhibitor molecules as obtained from in-situ Fourier transform infrared spectroscopy (FTIR) and density functional theory (DFT) calculations will be discussed. Area-selective ALD of SiO_2 using acetylacetone (Hacac) as inhibitor will be described as a model system, illustrating various mechanisms that can contribute to the loss of selectivity. It was found that at saturation, Hacac adsorbs through a mixture of chelate and monodentate bonding configurations. Hacac in monodentate configuration is displaced from the surface when exposed to bis(diethylamino)silane precursor molecules, which limits the selectivity. Strategies for improving the selectivity based on the understanding from these studies will be discussed.

[1] A. Mameli, M.J.M. Merkx, B. Karasulu, F. Roozeboom, W.M.M. Kessels, and A.J.M. Mackus, ACS Nano **11**, 9303 (2017).

[2] A.J.M. Mackus, M.J.M. Merkx, and W.M.M. Kessels, Chem. Mater. **31**, 2 (2019).

9:40am **AP+2D+EM+PS+TF-MoM5 Area-Selective Deposition of TiO_2 using Isothermal Integrated Atomic Layer Deposition and Atomic Layer Etching in a Single Reaction Chamber***,* ***Gregory Parsons****, S.K. Song, H. Saare,* North Carolina State University **INVITED**

Several new approaches are emerging where chemical etching is being coupled with atomic layer deposition to achieve area-selective deposition of dielectrics and metals. During ALD, selectivity is generally lost when undesired nuclei form on the targeted non-growth surface. These undesired nuclei can sometimes be removed by periodic etching, improving the overall selectivity. However, it is not known to what extent these coupled deposition/etching sequences can proceed while maintaining good selectivity. As desirable deposition and etching reactions proceed, other changes in the process can occur to enhance unwanted nucleation and/or impede desired etching, thereby limiting the net selectivity. Recent experiments in our lab have used in-situ probes to explore coupled thermal ALD and ALE super-cycles, performed sequentially under isothermal conditions in a single reaction chamber, to achieve area selective deposition of TiO_2 on SiO_2 with hydrogen-terminated silicon (100) as the desired non-growth surface. We find that as ALD/ALE super-cycles proceed, small changes occur in the ALD and ALE reactions, particularly during the transition from ALD to ALE, or from ALE to ALD. Also, modeling studies allow us to quantitatively analyze the ASD results and compare our findings to other known approaches. These insights will be helpful to understand opportunities and challenges in advanced atomic scale reactions and process implementation.

---

[1] **Paul Holloway Award Winner**

10:40am **AP+2D+EM+PS+TF-MoM8 Area-Selective Atomic Layer Deposition of Metal Oxides on an Inhibitor-Functionalized SiO_2 Surface*, Wanxing Xu,*** Colorado School of Mines*; P.C. Lemaire, K. Sharma, D.M. Hausmann,* Lam Research Corporation*; S. Agarwal,* Colorado School of Mines

The continued downscaling of modern semiconductor devices together with the incorporation of 3D architectures places new constrains on conventional lithography techniques. To enable further advances in patterning process, new techniques will be required for next-generation devices to overcome the challenges of limiting the growth of desired materials in a specific area. One method to address these issues is area-selective atomic layer deposition (ALD), which provides the opportunity to build defined patterns from the bottom-up at the atomic-level accuracy. In this study, we will focus on area-selective ALD of metal oxides including ZrO_2 and Al_2O_3 with a metal as the growth surface and inhibitor-functionalized SiO_2 as the non-growth surface. To inhibit ALD, the SiO_2 surfaces were functionalized with aminosilane inhibitors through the vapor phase or with a solution-based method. The functionalized SiO_2 surfaces were characterized by transmission Fourier transform infrared (FTIR) spectroscopy, ellipsometry, and water contact angle measurements. Metal oxides including ZrO_2 and Al_2O_3 were deposited by ALD using metal precursors and H_2O over a temperature range of 150-250 °C. *In situ* attenuated total reflection FTIR spectroscopy was utilized to identify the surface reactions sites and absorbed surface species during ALD. In addition, the corresponding film growth was measured using *in situ* four-wavelength ellipsometry.

Using *in situ* optical diagnostics, we show the mechanism for the breakdown in selectivity during area-selective ALD on a SiO_2 surface that is functionalized with aminosilanes. The infrared spectra show that aminosilane inhibitors react with almost all of the surface –SiOH groups forming Si–O–Si–R bonds on the surface (see Figure 1). After repeated exposure of the functionalized SiO_2 surface to TEMAZ and ZTB, these precursors react with Si–O–Si bonds without surface –SiOH groups (see Figure 2). Although small growth in the first few ALD cycles is not detected by *in situ* ellipsometry, growth inhibition breaks down after an increased number of ALD cycles. These results suggest that it is an additional requirement to suppress other reactions with a higher activation energy barrier during ALD expect removing main surface reactive sites through surface functionalization. To further impede growth of metal oxides on functionalized SiO_2 surface, a two-step functionalization method was developed to passivate the SiO_2 surface while providing additional steric blocking for the underlying substrates. Comparative studies were carried out to evaluate the effect of different functionalization methods on suppressing the nucleation during ALD.

11:00am **AP+2D+EM+PS+TF-MoM9 Area-selective Deposition Achieved in a Continuous Process using Competitive Adsorption*, Taewon Suh***, *Y. Yang, K.U. Lao, R.A. DiStasio, Jr., J.R. Engstrom,* Cornell University

A significant challenge for single-nm fabrication technologies is the development of area selective deposition (ASD) processes, particularly for device structures with exposed metallic and dielectric surfaces on patterned, often three dimensional, substrates. A number of techniques have been proposed and examined for ASD processes, particularly with respect to ALD, and these include the use of “permanent” blocking layers in the form of SAMs, and repetitive deposition/etch cycles. Some success has been reported with these techniques, but they possess potential drawbacks. An ideal ASD process should be fast, preferably vapor phase, and leave no residue on the non-growth surface. One technique that can possibly provide this is the use of competitive adsorption to induce area selective deposition, where a co-adsorbate is chosen that will bind much more strongly to one surface vs. another. A significant challenge concerning this approach is avoiding direct reactions between the co-adsorbate and the thin film precursor in the case of ALD, and also the co-reactant in the case of CVD. We are coupling quantum mechanical calculations of co-adsorbate/thin-film precursor/substrate interactions with experiments using our coupled micro-reactor/UHV surface analysis system. We have examined the effect of a class of unsaturated hydrocarbons as co-adsorbates on the CVD growth of ZrO_2 thin films using a Zr amido-coordination complex as the thin film precursor and O_2 as the co-reactant. The substrates were SiO_2 and Cu, and we examined the effects of both temperature, T_s = 120-240 °C, and the partial pressure of the co-adsorbate hydrocarbon. DFT calculations predict that the binding energies of these hydrocarbons are at least a factor of two larger on Cu vs. those on SiO_2. For CVD growth of ZrO_2 thin films as thick as 22 nm (growth rates of ~ 1 nm-s^{-1}), we find that the co-introduction of the hydrocarbon results in linear growth with time on a SiO_2 substrate, with no apparent incubation time, while essentially no growth is observed on Cu. *In situ*, post-deposition analysis with XPS reveals ZrO_2 thin films on SiO_2, and only adventitious carbon and less than a monolayer of Zr on the Cu surface. Consistent with a model based on competitive adsorption, we find that selectivity is eventually lost at sufficiently high substrate temperatures or sufficiently low partial pressures of the hydrocarbon co-adsorbate. Finally, we will report on the CVD growth on patterned Cu/SiO_2 substrates where we observe deposition only on those areas covered by SiO_2. We will conclude with a discussion of the promise and challenges of this approach for ASD concerning both ALD and CVD processes.

11:20am **AP+2D+EM+PS+TF-MoM10 Surface Chemistry during Plasma-Assisted ALE: What Can We Learn from ALD?*, Sumit Agarwal,*** Colorado School of Mines **INVITED**

Due to ever decreasing device dimensions and the introduction of 3D device architectures, it is challenging to operate within a narrow processing window using conventional plasma etching. One method to address the demands of the next-generation of devices is atomic layer etching (ALE) which provides high fidelity, selectivity, and directionality, and layer-by-layer removal. Plasma-assisted ALE has been extensively studied for a variety of materials, including Al_2O_3, HfO_2, Si, and Si–based dielectrics. Plasma-assisted ALE of SiO_2 or SiN_x typically uses two sequential steps in a cyclic fashion: CF_x deposition from a C_4F_8/Ar plasma followed by an Ar plasma activation step. However, the surface chemistry during plasma ALE is not well understood. In this study, we used *in situ* attenuated total reflection Fourier transform infrared (ATR–FTIR) spectroscopy and *in situ* four-wavelength ellipsometry during ALE to monitor the surface reactions, film composition, as well as the net film thickness. Similar to area-selective atomic layer deposition, we show that surface functionalization prior to ALE can be used to alter the etch per cycle. Using this methodology, I will discuss how selective functionalization of SiO_2 or SiN_x can be used to alter the selectivity during plasma-assisted ALE.

2D Materials
Room A226 - Session 2D+AP+EM+MI+MN+NS+PS+TF-MoA

Nanostructures including Heterostructures and Patterning of 2D Materials

Moderator: Deep Jariwala, University of Pennsylvania

1:40pm **2D+AP+EM+MI+MN+NS+PS+TF-MoA1 Tailoring and Patterning 2D Material Interfaces Through Chemical Functionalization*, Arend van der Zande,*** University of Illinois at Urbana-Champaign **INVITED**

Two-dimensional materials are all surface, so any change in the surface chemistry affects the entire material. This offers a challenge and an opportunity to engineering the material properties and new device behavior. There are many strategies to altering the chemical structure of 2D materials, yet one of the most successful is the chemical functionalization with low energy plasmas such as hydrogen and fluorine. Functionalization enables phase changes within materials to dramatically alter their properties, can be applied post synthesis and device fabrication, and is compatible with lithography for spatial patterning. Most studies of chemical functionalization focus on single functionalization of single 2D materials, yet there are many opportunities when applying the principles of chemical functionalization to spatially engineer the properties though in plane interfaces or out of plane in heterostructures.

First, we will examine selective etching with XeF_2 to pattern heterostructures using graphene etch stops. These techniques are self-limiting, yet scalable, and enable the patterning of 2D heterostructures into 3D multilayer circuitry. Moreover, devices like encapsulated graphene transistors fabricated with these techniques have exceptionally low contact resistances and mobilities which approach theoretical limits.

Second we will present a new strategy for tailoring the stoichiometry of functionalized graphene compounds through the systematic control of the ratio between adatoms. We demonstrate new ternary HFG compounds and reversible switching of material stoichiometry via the sequential exposure of graphene to low energy H plasma and XeF_2 gas. By patterning regions of different functionalization on a single chip, we perform direct comparisons and show spatially controlled tuning of the relative surface properties such as wettability, friction, electronic conductivity and molecular adhesion. Taken together, these studies show that chemical functionalization offers new atomically precise nanofabrication and materials engineering techniques for scalable engineering of circuitry along all three dimensions.

2:20pm **2D+AP+EM+MI+MN+NS+PS+TF-MoA3 Dual-Route Hydrogenation of the Graphene/Ni Interface*, Rosanna Larciprete,*** CNR-Institute for Complex Systems, Roma, Italy*; D. Lizzit,* Elettra - Sincrotrone Trieste, Trieste, Italy*; M.I. Trioni,* CNR-Institute of Molecular Science and Technologies, Milano, Italy*; P. Lacovig, L. Bignardi, S. Lizzit,* Elettra - Sincrotrone Trieste, Trieste, Italy*; R. Martinazzo,* Università degli Studi di Milano, Milano, Italy

Although the high surface-to-weight ratio would make graphene (Gr) one of the most promising material for hydrogen accumulation, up to now only moderate gravimetric density values of 1-2% have been obtained at room temperature (RT). The ultimate H coverage is limited by the competition between the adsorption and desorption/abstraction processes and by the elastic energy that accumulates in the C lattice once puckered by the local sp3rehybridization of the C atoms binding hydrogen. Moreover, for epitaxial Gr on metals, the substrate-induced Gr corrugation might modulates periodically H adsorption. In this respect, the Gr/Ni(111) interface appears much more favorable than other graphene/metal systems, as the limitations due to the presence of the moirè supercell vanish due to commensurate relation between the Gr and Ni(111) lattices. Moreover, hydrogenation might be favored by the peculiar reactivity of Gr/Ni(111).This issues motivated a re-investigation of the interaction of this particular interface with hydrogen.

In this study [1]we used x-ray photoelectron spectroscopy (XPS) and near edge x-ray absorption fine structure spectroscopy (NEXAFS) to follow the RT hydrogenation of Gr/Ni(111) and determined the configuration of the hydrogenated interface by scanning tunneling microscopy (STM). We found that hydrogenation proceeds through a dual path that includes hydrogen chemisorption on top of the graphene followed by a slow but continuous intercalation below graphene. At low coverage H atoms predominantly adsorb as monomers and chemisorption saturates when ≈ 25% of the surface is hydrogenated. The formation of C−H bonds determines new components in the C 1s core level spectrum that are attributed by DFT calculations to C atoms directly bonded to H and to their first neighbors. In parallel with chemisorption, with a much lower rate, H atoms intercalate below Gr and bind to Ni surface sites. Thermal programmed desorption measurements showed that chemisorbed hydrogen is released around 600 K, whereas the intercalated phase desorbs abruptly slightly below 400 K. Then the Gr cover, besides offering a storage volume for the intercalated H, stabilizes it above room temperature rising by a few tens of kelvins the H2 release temperature with respect to the bare Ni(111) surface.

The effectiveness of these results can be expanded by using Ni substrates with large specific surface, as nanoparticles or nanostructured foils, which, when covered with Gr, might become media where hydrogen can be loaded and stored above room temperature.

[1] D. Lizzit et al. ACS Nano 13 (2019) 1828

2:40pm **2D+AP+EM+MI+MN+NS+PS+TF-MoA4 Assembly of Arrays of Predefined Monolayer Features into vdW Heterostructure by a Continuous Exfoliate-align-Release Process*, Vu Nguyen,*** *H. Taylor,* University of California at Berkeley

One of the major challenges of van der Waals (vdW) integration of 2D materials is the high-yield and -throughput assembly of pre-defined sequence of monolayers into heterostructure arrays. Although a variety of techniques have been developed to exfoliate the 2D materials from the source and deterministically place them onto a target substrate, they typically can transfer only either a wafer-scale blanket or a small flake at a time with uncontrolled size and shape. Here we present a method to exfoliate arrays of lithographically defined monolayer MoS_2 and WS_2 features from multilayer sources and directly transfer them in a deterministic manner onto target substrates. The continuous exfoliate-align-release process, without the need of an intermediate carrier substrate, was enabled by a new transfer medium fabricated by spin-coating a low-crosslinked and transparent adhesive on a transparent, electrostatically active backing material with low surface energy. MoS_2/WS_2 vdW heterostructure arrays produced by this method were characterized, showing coupled photoluminescence between the monolayers. Light-emitting devices using WS_2 monolayer were also demonstrated, proving the functionality of the fabricated materials. This method promises to produce large-area monolayer and multiplex heterostructure arrays with capability to integrate with existing semiconductor manufacturing equipment.

3:00pm **2D+AP+EM+MI+MN+NS+PS+TF-MoA5 van der Waals Heterojunction Photothermoelectric Effect in MoS_2/Graphene Monolayers*, Yunqiu Kelly Luo,*** The Ohio State University*; T. Zhou,* University at Buffalo, State University of New York*; M. Newburger,* The Ohio State Univesity*; R. Bailey-Crandell, I. Lyalin,* The Ohio State University*; M. Neupane,* U.S. Army Research Laboratory*; A. Matos-Abiague,* Wayne State University*; I. Zutic,* University at Buffalo, State University of New York*; R. Kawakami,* The Ohio State University

Two-dimensional (2D) van der Waals (vdW) heterostructures provide a vast playground for exploring new phenomena due to its unique ability to tailor and combine dissimilar materials with atomic precision. In particular, the combination of graphene and transition metal dichalcogenides (TMDC) garners immense interest due to their novel optoelectronic, valleytronic and spintronic properties. Here, we report the observation of a highly tunable vdW heterojunction photothermoelectric effect (HPTE) in dual-gated MoS_2/graphene heterostructures, identified by a signature six-fold photocurrent pattern as a function of heterojunction bias and carrier density. In stark contrast to photovoltaic and photothermionic effects, we discover a new mechanism arising from photoexcitation of hot electrons in graphene and subsequent thermoelectric transport across the vdW junction. While analogous to lateral photothermoelectric effects at quasi-1D junctions in single layers, the vertical geometry of HPTE offers area scaling of 2D active regions and establishes, for the first time, the photothermoelectric response in vdW heterostructures. Operating at both low (18 K) and room temperatures, the discovery of HPTE creates new

possibilities for electrically-tunable broadband photodetectors and atomically-thin spin caloritronic devices.

3:20pm **2D+AP+EM+MI+MN+NS+PS+TF-MoA6 Formation of Edge-bonded MoS_2-graphene Nanoribbons by On-surface Synthesis***, **Mark Haastrup**, M. Mammen, J. Rodríguez-Fernández, J.V. Lauritsen,* Aarhus University, Denmark

2D materials exhibiting unique material properties have the potential for a huge impact on our future. Graphene, as the first discovered truly 2D material, has been extensively studied. However, the lack of an intrinsic band gap makes it inadequate for electronic and optical devices. MoS_2 from the family of transition metal dichalcogenides has been intensively investigated for its possibility to be used in future applications. The vision is to integrate various 2D materials to realise an actual device. However, the actual assembly of these materials with high controllability remains a challenge. Vertical heterostructures, supported by Van der Waals interactions, have already been realised by manually stacking 2D materials on top of each other[1]. An ultimate thin device can be realised by creating lateral heterostructures with atomically sharp interfaces where each material is directly bonded to another. Currently, methods for in-plane bonding of MoS_2 to other materials (e.g. graphene) are limited due to poor structural match. One possible solution is to develop selective bottom-up methods for synthesis of molecular nanostructures by self-assembly.

This study aim to investigate the fundamental nature of bonding of graphene nanoribbons (GNRs) to the edges of MoS_2 nanoparticles by scanning tunnelling microscopy (STM). The aim is to synthesise GNRs from precursor molecules through a thermally activated Ullmann reaction already used elsewhere[2,3]. After initial growth of MoS_2, it is necessary to anneal in a hydrogen atmosphere to activate the edges to facilitate the attachment of an intermediate structure of poly(para-phenylene) (PPP) wires. STM reveals the PPP wires have an affinity for the corners of the MoS_2 nanoparticles with a distance, obtained from line scans across the adsorption site, consistent with a covalent C-S bond.

[1]: Pant et al., Nanoscale, 2016, 8, 7, 3870-3887

[2]: Cai et al., Nature, 2010, 466, 7305, 470–473

[3]: Basagni et al., J. Am. Chem. Soc., 2015, 137, 5, 1802-1808

4:00pm **2D+AP+EM+MI+MN+NS+PS+TF-MoA8 The Effects of Metal-modification and Two Dimensional (2D) Lamellar Structure on Catalytic Performance of MFI Zeolite for Ethylene Conversion into Liquid Aromatics***, **Laleh Emdadi**, L. Mahoney, D. Tran, I. Lee,* US Army Research Laboratory

The effects of two dimensional (2D) meso-/microporous structure and metal modification with gallium or zinc on catalytic performances of lamellar MFI zeolites in ethylene conversion reaction to liquid aromatics were investigated. Dual template technique was used to synthesize the 2D zeolite and metal modification of the zeolite was carried out by wet impregnation method. The results of multiple analysis techniques such as TEM, XRD, Ar adsorption-desorption, UV-Visible spectroscopy, and H_2-TPR showed that the zeolite structure is a pivotal factor for controlling the type of metal dopant species forming on zeolite, their size, and their distribution. Adding metal dopants to 2D zeolite structures improved the yield of liquid aromatics and selectivity for mono-benzene alkylated aromatics compared to their microporous commercial MFI analogies while decreased the coke formation rate. Zinc loaded lamellar MFI had the most efficient catalytic performance among all studied catalysts with lowest amount of total coke and highest fraction of light coke including mono-benzene alkylated aromatics determined by combination of different techniques such as FTIR, UV-Vis, MS-temperature programmed oxidation (TPO), FTIR-TPO, and GC-MS. This can be explained by higher accessibility of reactants to active sites and facilitated transport of products and coke precursors from lamellar structure of this zeolite and the lower Brønsted/Lewis acid site ratio of this catalyst provided by metal modification which is more suitable for ethylene aromatization and suppresses the formation of heavy coke species. The catalytic performance of zeolite catalyst can be tuned by modulating both the textural and acidity properties of the zeolite structure. The metal modified 2D lamellar MFI zeolites as bifunctional catalysts open an avenue for converting large reactant molecules to desired products by designing a catalyst with an optimal structure, acidity, and dispersion of metal dopants.

4:20pm **2D+AP+EM+MI+MN+NS+PS+TF-MoA9 Structural Stability of Graphene Nanoflakes:From the View Point of Aromaticity***, M. Ushirozako, H. Matsuyama, A. Akaishi, **Jun Nakamura**,* The University of Electro-Communications (UEC-Tokyo), Japan

Recently, nano-scale graphene nanoflakes (GNFs) have attracted great attention as one of the promising materials for electronics and spintronics. Kim *et al*. have successfully fabricated GNFs with various sizes up to 35 nm and have reported that the photoluminescence property of GNFs depends on the size and the edge shape [1]. From the view point of the structural stability of GNFs, we have not yet acquired the systematic comprehension with regard to effects of shapes and sizes of GNFs on the stability. In the present study, we have examined how the stability of GNFs is dominated by the edge shape and the size of GNFs, using first-principles calculations within the density functional theory.

In order to evaluate the stability of GNFs, we calculated the edge formation energy. First, we consider GNFs with the six-fold symmetry (D_{6h}) and classify them into zigzag GNFs (ZZGNFs) and armchair GNFs (ACGNFs). ACGNFs have two subtypes, AC(1) and AC(2), depending on whether carbon atoms are just at the corner of the outermost envelope hexagon of GNFs. We define the edge purity as the ratio of the number of carbon atoms at the edge unambiguously regarded as the armchair to the total number of edge atoms. The purity of AC(1) is higher than that of AC(2). The chemical formulae associated with ZZ, AC(1), and AC(2) are $C_{6n^2}H_{6n}$, $C_{18n^2-18n+6}H_{12n-6}$, $C_{18n^2-30n+12}H_{12n-12}$, respectively. In addition, we also evaluate the structural stabilities of triangular and rhombus GNFs.

We calculated the edge formation energy of the GNFs having up to 1200 carbon atoms as a function of the number of edge carbon atoms [3]. The formation energy of ZZGNFs is higher than that of ACGNFs irrespective of the size of GNFs. This instability of ZZGNFs is attributed to the presence of the so-called edge state. Indeed, it has also been shown that the formation energy of the zigzag graphene nanoribbon is higher than that of the armchair one [4]. It is noted that AC(2) is slightly more stable than AC(1), whereas the purity of AC(2) is lower than that of AC(1). Such peculiar stabilization can be reasonably explained in terms of the aromaticity of GNFs. The Nucleus Independent Chemical Shifts (NICS) values, which is averaged for the six-membered rings in GNFs, for AC(2) are lower than those for AC(1). This means AC(2) is more aromatic than AC(1). We will discuss the quantitative relationship between the stability and the aromaticity of GNFS.

[1] S. Kim et al., ACS Nano, **6**, 9, 8203 (2012)

[2] W. Hu *et al*., J. Chem. Phys. **141**, 214704 (2014)

[3] A. Akaishi, M. Ushirozako, H.Matsuyama, andJ.Nakamura, Jpn.J.Appl.Phys. **57**, 0102BA(2018)

[4] S. Okada. Phys. Rev. B, **77**, 041408 (2008)

4:40pm **2D+AP+EM+MI+MN+NS+PS+TF-MoA10 Wafer-scale 2D-3D Mixed Heterostructures Enabled by Remote Epitaxy through Graphene***, **Jeehwan Kim**,* Massachusetts Institute of Technology **INVITED**

The current electronics industry has been completely dominated by Si-based devices due to its exceptionally low materials cost. However, demand for non-Si electronics is becoming substantially high because current/next generation electronics requires novel functionalities that can never be achieved by Si-based materials. Unfortunately, the extremely high cost of non-Si semiconductor materials prohibits the progress in this field. Recently our team has invented a new crystalline growth concept, termed as "remote epitaxy", which can copy/paste crystalline information of the wafer remotely through graphene, thus generating single-crystalline films on graphene [1,2]. These single-crystalline films are easily released from the slippery graphene surface and the graphene-coated substrates can be infinitely reused to generate single-crystalline films. Thus, the remote epitaxy technique can cost-efficiently produce freestanding single-crystalline films including III-V, III-N, and complex oxides. This allows unprecedented functionality of flexible device functionality required for current ubiquitous electronics. I will also present detailed mechanism behind remote atomic interaction through graphene [2]. In addition, we have recently demonstrated a manufacturing method to manipulate wafer-scale 2D materials with atomic precision to form monolayer-by-monolayer stacks of wafer-scale 2D material heterostructures [3]. In this talk, I will discuss the implication of this new technology for revolutionary design of next generation electronic/photonic devices with combination of 3D/2D mixed heterostructures.

[1] Y. Kim, et al, and J. Kim, "Remote epitaxy through graphene enables two-dimensional material based layer transfer" ***Nature***, Vol. 544, 340 (2017)

[2] W. Kong, et al, and J. Kim, "Polarity govern atomic interaction through two-dimensional materials", ***Nature Materials***, Vol. 17, 999 (2018)

[3] J. Shim, S. Bae, et al, and J. Kim, "Controlled crack propagation for atomic precision handling of wafer-scale two-dimensional materials" ***Science***, 362, 665 (2018)

2D Materials
Room A216 - Session 2D+AP+EM+MI+NS+PS+TF-MoA
2D Materials Growth and Fabrication

Moderator: Sarah Haigh, University of Manchester, UK

2:00pm **2D+AP+EM+MI+NS+PS+TF-MoA2 Synthesis of High Quality Monolayer Transition Metal Dichalcogenides using Direct Liquid Injection***, **Kathleen M. McCreary**, E.D. Cobas, A.T. Hanbicki, M.R. Rosenberger, H.-J. Chuang, B.T. Jonker,* U.S. Naval Research Laboratory

In recent years, interest in monolayer transition metal dichalcogenides (TMDs) has rapidly increased, spurred by the possibility for integration into a variety of technologies such as photodetection, flexible electronics, and chemical sensing. While fundamental investigations can be performed on exfoliated flakes or chemical vapor deposition synthesized isolated islands, the limited size resulting from these techniques poses a significant barrier forimplementation of TMDs in technological applications. To overcome these obstacles, new synthesis avenues should be explored. Here, we outline a novel technique that utilizes a commercially available Anneal Sys growth chamber equipped with direct liquid injection (DLI) heads for all precursors. The use of liquid, rather than solid precursors, provides fine control of both metal and chalcogen precursors leading to the synthesis of monolayer MoS_2 across cm^2 areas. Photoluminescence, Raman, XPS, and conductive AFM are used to evaluate DLI grown MoS_2, and indicate high quality material having low defect density, with metrics comparable to or better than exfoliated and chemical vapor deposition grown MoS_2.

2:20pm **2D+AP+EM+MI+NS+PS+TF-MoA3 Understanding and Controlling the Growth of 2D Materials with Non-Equilibrium Methods and in situ Diagnostics***, **David Geohegan**, Y-C. Lin, Y. Yu,* Oak Ridge National Laboratory*; C. Liu, G. Duscher,* University of Tennessee Knoxville*; A. Strasser,* University of Texas at Dallas*; A.A. Puretzky,* Oak Ridge National Laboratory*; K. Wang,* Intel Corporation, USA*; M. Yoon, C.M. Rouleau,* Oak Ridge National Laboratory*; S. Canulescu,* DTU Nanolab, Technical University of Denmark*; P.D. Rack,* University of Tennessee Knoxville*; L. Liang, W. Zhang, H. Cai, Y. Gu, G. Eres, K. Xiao,* Oak Ridge National Laboratory **INVITED**

Atomically-thin two-dimensional (2D) materials, including layered 2D transition metal dichalcogenide (TMD) semiconductors and their heterostructures, exhibit remarkable quantum properties that are envisioned for energy-efficient photovoltaics, flexible optoelectronics, catalysis, and quantum information science. However, significant synthesis and processing challenges currently limit the technologic development of these "all-surface" materials, including wafer-scale, bottom-up synthesis of uniform layers of crystalline 2D materials that are comparable in quality to exfoliated flakes of bulk materials. As-synthesized crystals of 2D TMDs display remarkable heterogeneity on both the atomistic level (e.g., vacancies, dopants, and edge terminations) and on the mesoscopic length scale (e.g., misoriented grains, layer orientations, and interactions with substrates and adsorbates) that can strongly influence the structure and electronic properties in 2D materials. This heterogeneity offers a serious challenge for synthesis and processing, yet offers a tremendous opportunity to tailor functionality.

Here we describe several approaches that are being developed for in situ diagnostic analysis and control of synthesis and heterogeneity. In addition to conventional vapor transport techniques, progress in laser-based approaches for 2D synthesis and modification, such as pulsed laser deposition (PLD) and pulsed laser conversion of precursors, are presented that permit control of the growth environment using time-resolved in situ diagnostics. The non-equilibrium advantages of PLD to form alloys and vertical heterojunctions are demonstrated using the tunable kinetic energy and digital nature of the process. Correlated atomic-resolution electron microscopy and atomistic theory are used to understand the size and stoichiometry of the "building blocks" deposited for synthesis and the forces that guide assembly. 2D crystals are grown directly on TEM grids within custom chambers and transmission electron microscopes where the ability to 'see' every atom in these atomically-thin crystals permits a unique opportunity to understand the forces governing their synthesis and functionality. In situ optical spectroscopy techniques are described to characterize the material's evolving structure and properties, offering the opportunity to 'close the loop' between synthesis and optoelectronic functionality of 2D materials and heterostructures.

Research sponsored by the U.S. Dept. of Energy, Office of Science, Basic Energy Sciences, Materials Science and Engineering Div. (synthesis science) and Scientific User Facilities Div. (characterization science).

3:00pm **2D+AP+EM+MI+NS+PS+TF-MoA5 Area-Selective Atomic Layer Deposition of 2D WS_2 Nanolayers***, **Shashank Balasubramanyam** [1],* Eindhoven University of Technology, The Netherlands, Noord Brabant*; M.J.M. Merkx,* Eindhoven University of Technology, The Netherlands*; W.M.M. Kessels,* Eindhoven University of Technology, The Netherlands, Netherlands*; A.J.M. Mackus,* Eindhoven University of Technology, The Netherlands, Nederland*; A.A. Bol,* Eindhoven University of Technology, The Netherlands, Netherlands

With continued downscaling of device dimensions, ultra-thin two dimensional (2D) semiconductors like WS_2 are considered as promising materials for future applications in nanoelectronics. At these nanoscale regimes, device fabrication with precise patterning of critical features is challenging using current top-down processing techniques. In this regard, area-selective atomic layer deposition (AS-ALD) has emerged as a promising candidate for bottom-up processing to address the complexities of nanopatterning. Till date, AS-ALD of metals[1] and dielectrics[2] have been successfully demonstrated. However, AS-ALD of 2D materials has remained elusive. In this contribution, we demonstrate area-selective deposition of 2D WS_2 nanolayers by using a three-step (ABC-type) plasma-enhanced ALD process.

AS-ALD of WS_2 was achieved by using acetylacetone (Hacac) inhibitor (A), bis(tertbutylimido)-bis(dimethylamido)-tungsten precursor (B), and H_2S plasma (C) pulses. This process resulted in immediate growth on SiO_2 while a significant nucleation delay was observed on Al_2O_3, as determined from *in-situ* spectroscopic ellipsometry (SE) and *ex-situ* X-ray photoelectron spectroscopy (XPS) measurements. The surface chemistry of this selective process was analysed by *in-situ* Fourier transform infrared spectroscopy (FTIR). The analyses revealed that the inhibitor adsorbed on the Al_2O_3 surface, blocking precursor adsorption, while little or no inhibitor adsorption was detected on the SiO_2 surface where WS_2 was readily deposited. Furthermore, the area-selective growth was demonstrated on SiO_2 samples with patterned Al_2O_3 on top. On SiO_2, WS_2 could be deposited with angstrom-level thickness control.

To improve the crystallinity, the AS-ALD WS_2 films were annealed at temperatures within the thermal budget of industrial semiconductor processing (≤ 450°C). The annealed films exhibited sharp Raman peaks, which is a fingerprint of highly crystalline WS_2. Furthermore, Raman line scans over the patterns showed very sharp peak intensity transitions at the SiO_2-Al_2O_3 interface which confirmed that annealing had no impact on selectivity.

To summarize, this work pioneered the combination of two key avenues in atomic-scale processing: area-selective growth and ALD of 2D materials. It is expected that the results of this work will lay the foundation for area-selective ALD of other 2D materials.

[1] R. Chen and S.F. Bent, *Adv. Mater.* (2006).

[2] A. Mameli, M.J.M. Merkx, B. Karasulu, F. Roozeboom, W.M.M. Kessels and A.J.M. Mackus, *ACS Nano* (2017).

3:20pm **2D+AP+EM+MI+NS+PS+TF-MoA6 Growth Behavior of Hexagonal Boron Nitride on Cu-Ni Binary Alloys***, **Karthik Sridhara**,* Texas A&M University*; J.A. Wollmershauser,* U.S. Naval Research Laboratory*; L.O. Nyakiti,* Texas A&M University*; B.N. Feigelson,* U.S. Naval Research Laboratory

Controlled growth of large area n-layered chemical vapor deposited (CVD) hexagonal boron nitride (h-BN) is of great interest as a tunnel dielectric, and substrate for graphene and transition metal dichalcogenides (TMDs). The CVD growth of h-BN has been demonstrated on various transition metal catalytic substrates such as Cu, Ni, Pt and Fe. Of these metal substrates, Cu and Ni are frequently used due to their relative abundance and low cost. However, h-BN growth on Cu leads to monolayer films, and growth on Ni yields thicker, substrate grain-dependent films. Therefore, a

[1] **TFD James Harper Award Finalist**

cost-effective transition metal substrate is needed that will facilitate controlled n-layered h-BN growth.

In this work, we prepare isomorphous Cu-Ni binary alloys from 10-90 wt.% Ni by creating Ni-rich (Ni-Cu) and Cu-rich (Cu-Ni) alloys using electroplating of Cu on Ni foils and Ni on Cu foils, respectively. The electroplated foils are then annealed at ~1030° C for >5 hours to create Ni-Cu and Cu-Ni alloys. The alloys are subsequently polished mechanically to create a planarized surface suitable for h-BN growth. The surface morphology before and after polishing is assessed using a scanning electron microscope (SEM). Energy dispersive spectroscopy (EDS) characterization of the alloys confirms a designed stoichiometry at every weight percent. h-BN is grown on the alloys using atmospheric pressure chemical vapor deposition (APCVD) at 1030° C, with ammonia borane as the precursor, and H_2/N_2 as the carrier gas flowing at ~200 sccm. Cu and Ni foils are used as control samples for this study. Fourier transform infrared reflection absorption spectroscopy (FT-IRRAS) is used to confirm and characterize h-BN growth directly on Cu, Ni and alloy substrates. SEM is performed to evaluate the h-BN film and crystal morphology. The results indicate that the h-BN growth behavior on Ni-Cu is different than on Cu-Ni alloys. A trend of decreasing h-BN amount with reducing Ni concentration is observed on Ni-Cu alloys while no such trend is observed on Cu-Ni alloys. Additionally, there are large (~20 µm) multilayer and monolayer single crystals of h-BN on Ni-Cu alloys, and predominantly monolayer crystals and films of h-BN on Cu-Ni alloys. The difference in growth behavior is studied using x-ray photoelectron spectroscopy (XPS) and electron backscattering diffraction (EBSD), which reveal that the alloy surface composition determines the h-BN growth. This work demonstrates how Cu-Ni alloy substrate of different compositions, along with CVD growth conditions, can be used to control h-BN growth.

4:20pm **2D+AP+EM+MI+NS+PS+TF-MoA9 Controlled Growth of Transition Metal Dichalcogenide Monolayers for Applications in Nanoelectronic and Nanophotonic Devices***, A. George, C. Neumann, D. Kaiser, R. Mupparapu,* Friedrich Schiller University Jena, Germany*; U. Hübner,* Leibniz Institute of Photonic Technology, Jena, Germany*; Z. Tang, A. Winter, I. Staude,* ***Andrey Turchanin,*** Friedrich Schiller University Jena, Germany

Controlling the flow rate of precursors is highly essential for the growth of high quality monolayer crystals of transition metal dichalcogenides (TMDs) by chemical vapor deposition. Thus, introduction of an excess quantity of precursors affects the reproducibility of the growth process and results in the multilayer growth. Here, we demonstrate the use of Knudsen-type effusion cells for controlled delivery of sulfur precursor for the large area, high density, size-controlled and highly reproducible growth of monolayer TMD crystals [1]. The size of the grown crystals can be tuned between 10 - 200 µm. We grow MoS_2, WS_2, $MoSe_2$ and WSe_2 monolayer crystals as well as $MoSe_2$-WSe_2 lateral heterostructures and characterize them by optical microscopy, atomic force microscopy, Raman spectroscopy, photoluminescence spectroscopy and electrical transport measurements. It has been found that they possess a high crystalline, optical and electrical quality based on their single crystalline nature. We demonstrate their implementation in novel field-effect and nanophotonic devices and discusse an influence of the point defect density on their functional characteristics [2-3]. Moreover, we present a novel synthetic route for the integration of TMDs into lateral heterostructures with other 2D materials [4].

[1] A. George et al., *J. Phys.: Mater.* 2 (2019) 016001.

[2] T. Bucher et al., *ACS Photonics* 6 (2019) 1002.

[3] R. Meyer et al., *ACS Photonics* 6 (2019) DOI: 10.1021/acsphotonics.8b01716

[4] A. Winter et al., *Carbon* 128 (2018)106.

4:40pm **2D+AP+EM+MI+NS+PS+TF-MoA10 Atomic Layer Deposition of BN as a Novel Capping Barrier for B_2O_3*, Aparna Pilli,*** *J. Jones, J.A. Kelber,* University of North Texas*; A. LaVoie, F. Pasquale,* Lam Research Corporation

The deposition of boron oxide (B_2O_3) films on Si and SiO_2 substrates by atomic layer deposition (ALD) is of growing interest in microelectronics for shallow doping of high aspect ratio transistor structures. B_2O_3, however, forms volatile boric acid (H_3BO_3) upon ambient exposure, requiring a passivation barrier, for which BN was investigated as a possible candidate. Here, we demonstrate, deposition of BN by sequential BCl /NH reactions at 600 K on two different oxidized boron substrates: (a) B O deposited using BCl /H O ALD on Si at 300 K (“B O /Si”); and (b) a boron-silicon oxide formed by sequential BCl /O reactions at 650 K on SiO followed by annealing to 1000 K (“B-Si-oxide”). X-ray photoelectron spectroscopy (XPS) data demonstrate layer-by-layer growth of BN on B_2O_3/Si with an average growth rate of ~1.4 Å/cycle, accompanied by some B_2O_3 removal during the first BN cycle. In contrast, continuous BN growth was observed on B-Si-oxide without any reaction with the substrate. XPS data also indicate that the oxide/nitride heterostructures are stable upon annealing in ultrahigh vacuum to >1000 K. XPS data, after the exposure of these heterostructures to ambient, indicate a small amount of BN oxidation at the surface NH species, with no observable hydroxylation of the underlying oxide films. These results demonstrate that BN films, as thin as 13 Å, are potential candidates for passivating boron oxide films prepared for shallow doping applications.

5:00pm **2D+AP+EM+MI+NS+PS+TF-MoA11 Atomic Layer Deposition of SiO_2 on Group VIII Metals: Towards Formation of a 2D Dielectric***, T. Suh, R. Yalisove,* ***James Engstrom,*** Cornell University

The atomic layer deposition (ALD) of many metals, particularly Group VIII (now known as Groups 8, 9 and 10), on SiO_2 has been an active area of research in many fields, which include microelectronics and heterogeneous catalysis. There have been many fewer studies of the inverse—the deposition of SiO_2 on many of these same metals. One possible reason to explore the ALD growth of SiO_2 on transition metals is that it might provide a route to an atomically thick SiO_2 dielectric, *silicatene*. Silicatene is a 2D material that consists of a bilayer of Si_2O_3 linked to each other by bridging oxygen atoms (giving SiO_2), where there are no dangling bonds or covalent bonds to the underlying substrate on which it is grown. For example, an established route to form silicatene involves deposition of elemental Si in UHV and subsequent high-temperature annealing on various single-crystalline metal surfaces including, but not limited to, Ru(0001), Pt(111), and Pd(100). Such a process, unfortunately, is likely not compatible with high-volume manufacturing. With this motivation we embarked on a study of the plasma-assisted ALD of SiO_2 on e-beam deposited polycrystalline thin films of Ru, Pt and Pd using a commercial ALD reactor. We analyzed both the thin films and the starting substrates using a combination of techniques including contact angle, spectroscopic ellipsometry (SE) and X-ray photoelectron spectroscopy. Thin films of SiO_2 were deposited using tris(dimethylamido)silane and an oxygen plasma at a substrate temperature of 200 °C, and we examined growth for 5, 10, 20, 50 and 100 cycles. Contact angle measurements showed immediate evidence for SiO_2 deposition on all metal surfaces, and the contact angle decreased and remained constant and < 10° from 5 to 100 cycles of ALD. From SE we found little evidence of an incubation period, and growth was linear for the range of sample examined and the thickness deposited per cycle was remarkably constant at a value of 0.76-0.78 Å-cycle^{-1}. Analysis of these films using angle-resolved XPS was consistent with the formation of a thin film of SiO_2 with uniform thickness. Having characterized the thin film thickness-ALD cycle relationship we subjected SiO_2 thin films with thickness of ~ 7-15 Å to post-deposition high-temperature anneals in oxygen furnace. Initial attempts to form silicatene with an anneal at 800 °C, produced a structure suggesting possible interfacial reaction between the SiO_2 and Ru, perhaps involving silicide formation. We will end our presentation with a discussion of recent work involving a more extensive examination of the post-deposition annealing step, and deposition on patterned wafers.

Thin Films Division
Room A124-125 - Session TF+2D+AP+EL+SS-MoA
ALD and CVD: Nucleation, Surface Reactions, Mechanisms, and Kinetics

Moderators: Adrie Mackus, Eindhoven University of Technology, The Netherlands, Qing Peng, University of Alabama

1:40pm **TF+2D+AP+EL+SS-MoA1 ALD on Particles: What is Different from Wafers?***,* ***Ruud van Ommen,*** Delft University of Technology, Netherlands **INVITED**

Advanced materials, often relying on nanostructured particles as building blocks, are crucial in meeting grand challenges in energy and health. Atomic layer deposition (ALD) is an excellent technique to make such nanostructured particles: particles of which the surface is either covered by an ultrathin film or by nanoclusters. Although the underlying mechanisms are similar, there are quite some differences between ALD processing of wafers and ALD processing of particles. This presentation will discuss recent developments and insights in the field of applying ALD to particles, with an emphasis on reactor technology, precursor utilization, operating conditions, and scaling up. I will show that ALD is suited to produce

nanostructured particles with very high precision. Moreover, it is scalable such that large amounts of such particles can be produced.

2:20pm **TF+2D+AP+EL+SS-MoA3 Insights into Particle ALD Peculiarities from In- and Ex-Situ Characterization***, **Benjamin Greenberg**,* American Society for Engineering Education*; J.A. Wollmershauser, B. Feygelson,* U.S. Naval Research Laboratory

Particle atomic layer deposition (pALD) is an increasingly popular technique for mass production of core/shell nanoparticles (NPs). In a typical pALD process, NP powders are agitated in a fluidized bed or rotary reactor, and conformal coating of the entire powder surface—often > 100 m^2 in lab-scale reactors—is attempted via prolonged precursor exposures and purges. Over the past 2+ decades there have been many reports of highly encouraging results, including TEM images of NPs individually encapsulated by shells of uniform thickness. Nevertheless, several fundamental questions about pALD mechanisms and behavior remain challenging to answer. For example, how does the pALD growth per cycle (GPC) deviate from the corresponding ALD GPC on a flat substrate, and why? Or more importantly, what conditions are required to maximize the fraction of powder that attains an ideal core/shell structure (individual NP encapsulation) rather than a coated-agglomerate structure in which cores are glued together? In this work, using a commercial rotary pALD reactor to coat various NPs with oxide shells, we employ a wide array of characterization techniques to shed light on these issues and inform process optimization. In situ, we experiment with relatively uncommon techniques such as high-speed video analysis and pyrometry of the agitated NP powder, as well as conventional techniques such as mass spectrometry (RGA). High-speed videos in particular reveal aspects of the process often undiscussed (and sometimes difficult to convey) in the pALD literature, including changes in the powder motion as surface chemistry evolves. Ex situ, we characterize the coated NPs via TEM, XRD, SAXS, XPS, and N_2-adsorption surface area measurements (BET method).

3:00pm **TF+2D+AP+EL+SS-MoA5 Controlling the Nucleation of CVD Cobalt Films on SiO_2 : Combining an Amido-based Nucleation Promotor with an Amine-based Growth Inhibitor to Afford Atomically-smooth Surfaces***, **Zhejun Zhang**, G.S. Girolami, J.R. Abelson,* University of Illinois at Urbana-Champaign

Cobalt films are of interest for the back-end metallization and transistor contact in microelectronics because cobalt has a greater electromigration resistance and a lower diffusion rate in dielectrics compared with copper. However, few-nanometer thick Co films deposited by CVD on dielectrics are usually non-continuous – they consist of islands with pinholes and significant roughness – which renders them unsuitable for nanoscale device fabrication. A nucleation layer, such as TiN, can be pre-deposited to improve the area density of Co nuclei; this approach eliminates the problem of islanding, but it subtracts cross-sectional area from the plug or line, thus increasing the electrical resistance.

Here, we solve the Co nucleation problem in CVD using a two-pronged approach. First we expose the SiO_2 surface to a tetrakis(dimethylamido)(transition metal) precursor at low temperature. This affords a self-limiting, submonolayer coverage of an intermediate, similar to the behavior of such molecules in ALD processes. The adsorbate layer then enhances the nucleation of cobalt from the $Co_2(CO)_8$ precursor, such that a large area density of nanoscale islands forms with essentially no nucleation delay. Using this approach, the rms surface roughness for a 1.5-nm-thick Co film decreases from 2.5 to 1.0 nm.

Second, we further improve the surface morphology by adding a co-flow of ammonia together with the carbonyl precursor; this serves as a growth inhibitor that reduces the steady-state growth rate of Co films by 50 %. The presence of the inhibitor does not alter the nucleation rate, however, the rms roughness of a 1.5-nm-thick film is further reduced to only 0.4 nm. We suggest that the roughness is due to a better valley-filling at low precursor reaction probability, consistent with the literature. In summary, our approach enables the use of CVD to afford excellent Co films for nanofabrication.

3:20pm **TF+2D+AP+EL+SS-MoA6 Plasma-assisted Atomic Layer Epitaxy of Indium Aluminum Nitride Studied Using *in situ* Grazing Incidence Small-angle X-ray Scattering***, **Jeffrey M. Woodward**,* ASEE (residing at US Naval Research Laboratory)*; S.G. Rosenberg,* American Society for Engineering Education (residing at US Naval Research Laboratory)*; S.D. Johnson, N. Nepal,* U.S. Naval Research Laboratory*; Z.R. Robinson,* SUNY Brockport*; K.F. Ludwig,* Boston University*; C.R. Eddy,* U.S. Naval Research Laboratory

Indium aluminum nitride (InAlN) is an attractive material for power electronic applications. However, conventional methods of epitaxial growth of InAlN are challenged by a large miscibility gap and the significant differences in optimal growth conditions for the constituent aluminum nitride (AlN) and indium nitride (InN) binary compounds. Despite these challenges, the epitaxial growth of InAlN alloys throughout the entire compositional range has been demonstrated using plasma-assisted atomic layer epitaxy (ALEp)[1], a variant of atomic layer deposition in which relatively higher temperatures are utilized. In the ALEp growth of InAlN, the desired alloy compositions are achieved by forming ultra-short period superlattices of alternating InN and AlN layers, referred to as digital alloys (DA). In order to further advance these empirical efforts, significant research is needed to better understand the nucleation and growth kinetics of ALEp DA growth. To this end, we employ *in situ* grazing incidence small angle X-ray scattering (GISAXS) for the real-time study of the evolving ternary InAlN surfaces as has been done previously for binary InN[2] and AlN[3].

Here we present *in situ* GISAXS studies of ALEp growth of InN, AlN, and a range of InAlN DAs on GaN (0001) substrates, which were performed at Brookhaven National Laboratory's NSLS-II using a custom reactor. The InAlN DAs studied include $In_{0.19}Al_{0.81}N$ (3 AlN cycles and 2 InN cycles per supercycle), $In_{0.5}Al_{0.5}N$ (1 AlN cycle and 3 InN cycles per supercycle), $In_{0.64}Al_{0.36}N$ (1 AlN cycle and 5 InN cycles per supercycle) and $In_{0.83}Al_{0.17}N$ (1 AlN cycle and 14 InN cycles per supercycle). Preliminary analysis of the data suggests that while the pure InN and AlN grew in 3D and 2D modes, respectively, the InAlN growth mode did not follow a simple trend as the nominal composition was tuned from InN to AlN. Instead, select compositions (50% and 83% In) exhibited predominantly 3D growth, while others (19% and 64% In) exhibited 2D growth. We also present complementary ALEp growth studies using a commercial Ultratech/Cambridge Nano Tech Fiji 200 and *ex situ* characterization methods, including high resolution X-ray diffraction, X-ray reflectivity, and atomic force microscopy.

[1] N. Nepal, V.R. Anderson, J.K. Hite, and C.R. Eddy, Thin Solid Films **589**, 47 (2015)

[2] J.M. Woodward, S.G. Rosenberg, A.C. Kozen, N. Nepal, S.D. Johnson, C. Wagenbach, A.H. Rowley, Z.R. Robinson, H. Joress, K.F. Ludwig Jr, C.R. Eddy Jr, J. Vac. Sci. Technol. A **37**, 030901 (2019)

[3] V.R. Anderson, N. Nepal, S.D. Johnson, Z.R. Robinson, A. Nath, A.C. Kozen, S.B. Qadri, A. DeMasi, J.K. Hite, K.F. Ludwig, and C.R. Eddy, J. Vac. Sci. Technol. A **35**, 031508 (2017)

4:00pm **TF+2D+AP+EL+SS-MoA8 Real-time Monitoring of the Surface Chemistry of Atomic Layer Deposition by Ambient Pressure X-ray Photoelectron Spectroscopy***, **Joachim Schnadt**, P. Shayesteh,* Lund University, Sweden*; R. Tsyshevskiy,* University of Maryland*; J.-J. Jean-Jacques, F. Bournel,* Sorbonne Université, France*; R. Timm,* Lund University, Sweden*; A.R. Head,* Brookhaven National Laboratory*; G. D'Acunto, F. Rehman, S. Chaudhary,* Lund University, Sweden*; R. Sánchez-de-Armas,* Uppsala University, Sweden*; F. Rochet,* Sorbonne Université, France*; B. Brena,* Uppsala University, Sweden*; A. Mikkelsen, S. Urpelainen, A. Troian, S. Yngman, J. Knudsen,* Lund University, Sweden **INVITED**

Atomic layer deposition (ALD) and chemical vapour deposition (CVD) are very important methods that enable a highly controlled growth of thin films [1]. The surface chemis-try of the underlying processes remains, however, little understood. While idealised reac-tion mechanisms have been developed, they represent postulates rather than models based on the factual identification of surface species and kinetics [2]. New *in situ* and *operando* methods offer the prospect of gaining a much more thorough understanding of the involved molecular and atomic surface processes and (dynamic) structures, which, in turn, means that a much better knowledge basis can be achieved for the future improvement of materials and growth recipes (see, e.g. [3,4]). One such *operando* method, which can be applied to the investigation of ALD and CVD, is synchrotron-based ambient pressure x-ray photoelectron spectroscopy (APXPS). While conventional x-ray photoelectron spectroscopy (XPS) is limited to vacuum pressures of 10^{-5} mbar and below, APXPS can be carried out at realistic pressure. Today,

most APXPS machines can operate at pressures up to the 10 mbar regime, which is an ideal match to the pressure regime used in standard ALD reactors.

Here, I will report on our recent efforts to apply density functional theory (DFT)-assisted synchrotron-based APXPS to the ALD/CVD of oxides (TiO_2, SiO_2, and HfO_2) on semiconductor (InAs and Si) and oxide surfaces (TiO_2, RuO_2) [3-5]. I will show that APXPS allows the identification of the surface species occurring during thin film growth and the real-time monitoring of their evolution with a time resolution of down into the millisecond regime. Here, DFT is an important tool for pinpointing the nature of the chemical species and for providing deeper insight in the surface chemical processes. I will also report on our efforts to further improve instrumentation with the goal of achieving a much closer match of the APXPS sample environment with the geometries used in conventional ALD reactors. The development will also open for the use of a wider range of precursors and growth protocols.

[1] V. Miikkulainen et al., J. Appl. Phys. 113 (2013) 021301.

[2] F. Zaera, Coord. Chem. Rev. 257 (2013) 3177.

[3] B. A. Sperling et al. Appl. Spectrosc. 67 (2013) 1003.

[4] K. Devloo-Casier et al., J. Vac. Sci. Technol. 32 (2014) 010801.

[3] S. Chaudhary et al. , J. Phys. Chem. C 119 (2015) 19149.

[4] A. R. Head et al. , J. Phys. Chem. C 120 (2016) 243.

[5] R. Timm et al., Nature Commun. 9 (2018) 412.

4:40pm **TF+2D+AP+EL+SS-MoA10 Kinetics during TMA-H_2O ALD: The Possible Role of Cooperative Surface Reactions***, **Brent Sperling**, B. Kalanyan, J.E. Maslar,* National Institute of Standards and Technology (NIST)

Until recently, the CH_3 groups produced by surface reactions of trimethylaluminum (TMA) during atomic layer deposition were widely believed to always be highly reactive toward H_2O, but *in situ* measurements have shown this is not the case below about 200 °C.[1] At these temperatures, some CH_3 groups react slowly, and a significant amount persists from cycle to cycle under typical growth conditions. Interestingly, these persistent CH_3 groups are not incorporated as carbon impurities. We have observed these CH_3 groups using *in situ* reflection infrared spectroscopy and have confirmed low carbon concentrations in our films using *ex situ* XPS. Furthermore, we have measured the kinetics of the reaction with H_2O and have found them to be well-described by a double-exponential decay function. A simple Monte Carlo simulation that incorporates cooperative effects by clustered surface reactants (as suggested by DFT calculations[2]) reveals that a double-exponential decay of coverage can result even when only one species of reactant is present. Furthermore, the short-range distributions of coverage that result in the simulation differ from purely random ones. This difference implies that measurements sensitive to dipole-dipole interactions when combined with an independent measurement of surface coverage could be used to confirm or disprove the cooperative reaction model.

[1] V. Vandalon and W. M. M. Kessels, *J. Vac. Sci. Techol. A***35** (2017) 05C313

[2] M. Shirazi and S. D. Elliott, *Nanoscale***7** (2015) 6311.

5:00pm **TF+2D+AP+EL+SS-MoA11 Atomic Layer Deposition of Metal Sulfides: Growth and Surface Chemistry***, **Xinwei Wang**,* Shenzhen Graduate School, Peking University, China

Atomic layer deposition (ALD) of metal sulfides has recently aroused great interest, and many new sulfide ALD processes have emerged during the past several years. Surface chemistry plays a key role in ALD, but it remains yet to be investigated for many recently developed sulfide ALD processes. In this representation, I will report our study on the growth and surface chemistry of the ALD of nickel, iron, and cobalt sulfides, using various in situ characterization techniques of X-ray photoelectron spectroscopy (XPS), low-energy ion scattering (LEIS), quartz crystal microbalance (QCM), and quadrupole mass spectrometry (QMS). For instance, nickel sulfide (NiS) can be deposited from a Ni amidinate precursor ($Ni(amd)_2$) and H_2S by ALD (*Chem. Mater.* (2016) 28, 1155), but the surface chemistry of this process is found to deviate from the conventional ligand-exchange ALD scheme, and a formation of a nonvolatile acid-base complex from acidic surface sulfhydryl and basic amidine is suggested during the H_2S half-cycle (*J. Phys. Chem. C* (2018) 122, 21514). The initial ALD growth of NiS on a SiO_x surface is also intriguing, as the initial growth mechanism is found to be rather different from that in the later steady film growth. In the initial ALD cycles, the XPS results show a drastic cyclic variation of the signals for the Ni−O bonds, with prominently observable Ni−O signals after each $Ni(amd)_2$ dose but almost negligible after the subsequent H_2S dose. These results suggest that the Ni−O bonds are first formed on the surface in the $Ni(amd)_2$ half-cycles and then mostly converted to NiS in the following H_2S half-cycles. To describe this initial ALD growth process, a reaction-agglomeration mechanistic scheme is proposed (*Chem. Mater.* (2019) 31, 445). Surface thermolysis study of the Ni amidinate precursor further reveals the temperature-dependent behavior of the film growth.

Electronic Materials and Photonics Division
Room A214 - Session EM+2D+AP+NS+PS-TuM

New Devices and Materials for Electronics and Photonics

Moderators: Sean W. King, Intel Corporation, Michelle M. Paquette, University of Missouri-Kansas City

8:00am **EM+2D+AP+NS+PS-TuM1 Performance Modeling and Design for Spintronic Logic and Memory Devices**, ***Azad Naeemi,*** Georgia Institute of Technology **INVITED**

As scaling conventional logic and memory devices becomes more and more challenging, there is a global search for novel materials and devices that can augment mainstream technologies used for data storage and processing. To this end, spintronic materials and devices are promising candidates as they provide dense non-volatile storing elements that enable novel computing paradigms such as in memory-computing and neural networks.

This talk will present physical models for various read and write spintronic mechanisms and quantifies the potential performances of Boolean circuits based on various spintronic logic devices. It will be shown that without major breakthroughs such circuits will not be able to compete with their CMOS counterparts. However, novel circuit paradigms that take advantage of the physics of these devices can potentially provide significant benefits. For example, cellular neural networks based on spintronic devices are projected to perform better compared to their analog CMOS implementation.

While spin-transfer-torque random access memory (STT-RAM) is becoming commercially available, it suffers from relatively large switching currents that limits its density and causes reliability challenges. Novel read and write mechanisms such as spin-orbit torque or magneto-electric effects can potentially address or partially mitigate some of these challenges. In this talk, the array-level potential performance of various magnetic memory devices will be quantified and benchmarked.

8:40am **EM+2D+AP+NS+PS-TuM3 High Yield, Low Variability HfO_2 1T1R Cells Fabricated in 65nm CMOS**, *J.H. Hazra, M.L. Liehr, K. Beckmann,* ***Nathaniel C. Cady,*** SUNY Polytechnic Institute

Hafnium Oxide (HfO_2) based Resistive Random Access Memory (ReRAM) devices are promising candidates for non-volatile memory, having a wide variety of applications in neuromorphic computing, artificial intelligence and future memory solutions. Stochastic conductive filament (CF) generation and rupture processes, however, contribute to high variability resistive switching in these devices. In order to address this issue, an extensive characterization of HfO_2 1 transistor 1 RRAM (1T1R) cells was performed to investigate switching yield and cell-to cell variability. 1T1R devices were integrated into a 300mm wafer platform utilizing the IBM 65nm 10LPe process technology, in which the memristor device stack is implemented between the M1 and M2 metallization layers, using a custom designed FEOL compatible process flow. The ReRAM device stack is comprised of a TiN bottom electrode followed by conformal deposition of the HfO_2 switching layer, Ti oxygen scavenging layer and TiN top electrode. The HfO_2 switching layer was deposited using an atomic layer deposition (ALD) process with an organic precursor. For statistical significance, the performance of 50 different 1T1R cells was compared for cell-to-cell variability in operating voltage and resistance in the on and off state. An impressive 100% switching yield and low cell-to-cell switching variability were observed for these devices. 1T1R cells were also investigated for long term endurance and high temperature retention, exhibiting excellent endurance of up to 1 billion switching cycles with an average R_{off}/R_{on} ratio of 10:1. As compared to 1T1R cells that we have fabricated with alternative ALD precursors/methods, these devices show superior yield and performance. We are currently performing compositional and structural comparisons between these sets of devices, to elucidate the impact of ALD precursor choice and processing methods on yield and electrical performance.

9:00am **EM+2D+AP+NS+PS-TuM4 Heat Transfer Proximity Effects in Resistive Memory Crossbar Arrays**, ***Marius Orlowski,*** *M.S. Al-Mamun,* Virginia Tech

Evidence for thermal cross talk in resistive RAM memory arrays is presented. Frequent switching of a resistive memory cell ($Cu/TaO_x/Pt$) may lead to a considerable local accumulation of Joules heat. The heat generated in a stressed device spreads via common electrode lines to the neighboring cells impacting their switching behavior. As a probe into degraded performance of the neighbor cells we choose the cell itself set into the on-state under specific conditions. The cell is set at a critical compliance current I_{cc} that allows repeated switching for no more than ~15 cycles. After the maximum number of cycles the on-state becomes volatile. For a lower I_{cc}, the cell produces a volatile on-state, and for higher I_{cc} the cell switches for hundred of times with a stable on-state. We find that the cells in close proximity of the heated device display various degrees of degradation indicated by a reduced number of cycles of the probed cell. The 1st neighbor cell experiences the greatest, and the 4th neighbor cell the smallest degradation. This indicates the spread of the heat from the heated device to its neighbors. After a sufficient cooling off period (10 minutes or longer), all the neighboring cells and the heated device display again the maximum number of cycles i.e. 15, when set under the critical compliance current and reset, repeatedly. Also cells that don't share any of the common electrode metal lines with the heated source cell, may degrade provided that the intermediate cells are set to on-state, thus enabling a continuous thermal conduction path between the heated cell and the probed cell. The heat dissipation from the heated device is slower for narrow and thin metal electrode lines than for wide and thick metal lines. However, in case of wide and thick metal lines more distant neighbor cells are affected by the parasitic cell-to-cell heat transfer.

We have performed the characterization o the neighboring cells along the Cu and Pt electrode lines. We find that the performance degradation of the neighboring cells along the Cu line is significantly stronger than along the Pt metal line. This observation is consistent with the much better heat conductivity of Cu lines (385W/(mK) and 150nm thick) than the Pt (72W/(mK) and 50nm thick) lines, but is at odds with the assumption of the standard electro-chemical metallization model postulating a conical shape of the Cu filament with a broad base of the cone at the Pt electrode and a tip at the Cu electrode. We discuss the extant controversial experimental evidence and models for the filament's shape and propose an hour-glass shape for the filament reconciling the extant findings and our thermal results.

9:20am **EM+2D+AP+NS+PS-TuM5 High Performance Memristive Action in Methylammonium Bismuth Iodide([MA]3Bi2I9) Films**, *P. Cheng,* Vanderbilt University*; G. Luo,* Washington University in St. Louis*; Z. Gao,* University of Central Florida*; A. Thind, R. Mishra,* Washington University in St. Louis*;* ***Parag Banerjee,*** University of Central Florida

We demonstrate high performance (ON/OFF ~ $2.4x10^5$) resistive switching in methylammonium bismuth iodide ($(CH_3NH_3)_3Bi_2I_9$ or, MBI) thin films.[1] MBI has a post-perovskite structure and consists of 2D layers of face-shared

BiI_6 octahedra. This talk focuses on the structure, composition and associated defect chemistry that is critical for memristive behavior in MBI films.

Memristors are formed by contacting MBI films with aluminum electrodes. The switching for a 200 nm film is observed at voltages ~ 0.5 V. High frequency performance of these memristors shows a peak ON/OFF ratio $2.4x10^5$at 50 KHz. The ON state retention is maintained at 50C for > 10^6 seconds. Stable room temperature endurance is noted for up to 1000 cycles. Energy dispersive x-ray spectroscopy on planar memristor devices show that, postswitching,

a detectable change in the I- concentration is observed closer to the anode side. Density-functional theory (DFT) calculations show low activation barrier for iodine migration in agreement with the experimental results. The DFT calculations also provide insights about the migration pathway and strategies to control this behavior.

From a synthesis perspective, MBI films can be deposited using solution as well as low temperature (< 200C), atmospheric CVD technique.[2] The compounds are air stable. This family of ternary compounds offers a large compositional and structural tunability; unlike binary metal oxides commonly used for memristors. As opposed to recent 2D MoS_2 based planar, tunneling RAM devices[3], the vertical stack of the 2-terminal memristor bodes well for scalability. Thus, we propose that hybrid organic-inorganic thin films may offer strategic materials and design advantages together with seamless process integration into current Si-based devices.

References:

1. Cheng, P., Thind, A., Gao, Z., Luo, G., Mishra, R., Banerjee, P., "High performance memristors from methylammonium bismuth iodide thin films", Submitted.

2. Chen, X.; Myung, Y.; Thind, A. S.; Gao, Z.; Yin, B.; Shen, M.; Cho, S. B.; Cheng, P.; Sadtler, B.; Mishra, R.; Banerjee, P., "Atmospheric pressure chemical vapor deposition of methylammonium bismuth iodide thin films", J. Mater. Chem. A, 2017, 5, 24728 - 24739.

3. Vu et al., "Two-terminal floating-gate memory with van der Waals heterostructures for ultrahigh on/off ratio", Nat. Comm., 2016, DOI: 10.1038/ncomms12725.

9:40am **EM+2D+AP+NS+PS-TuM6 Mechanism of Chalcogen Passivation of GaAs Surfaces***, **Takayuki Suga**, S. Goto,* UEC-Tokyo, Japan*; A. Ohtake,* NIMS, Japan*; J.N. Nakamura,* UEC-Tokyo, Japan

GaAs surfaces are stabilized by surface treatments with Se or S through the reduction of the dangling bond density [1,2]. It has long been thought that the Se- or S-treated GaAs(111)B-(1x1) surface has a simple structure; the outermost As atoms of the ideal (111)B surface are completely replaced by Se or S atoms, the Se- or S-terminated model [3]. In general, the structural stability of compound semiconductor surfaces can be explained in terms of the so-called electron-counting rule (ECR) [4]. The Se- or S-terminated model, however does not satisfy ECR. Recently, the atomic structure of the Se-treated GaAs(111)B surface has been revisited [5] and another structure model has been proposed, where the Se atoms substitute 3/4 of the topmost surface As atoms in a (2x2) unit [6]. This mixed Se/As-terminated model satisfies ECR, being electronically stable [6]. We have depicted phase diagrams of Se- or S- treated GaAs(111)B surface at 0K as functions of the chemical potentials of Se ($\Delta\mu_{Se(S)}$) and As ($\Delta\mu_{As}$). The (2x2) As-trimer and the mixed Se(S)/As-terminated surfaces appear under Se poor condition. It is noted that the Se- or S-terminated surface also becomes stable as $\Delta\mu_{Se}$ or $\Delta\mu_{S}$ increases, respectively, even though these surfaces are not qualified for ECR.

The Se(S)-treated GaAs(111)B surface is prepared experimentally by molecular beam epitaxy under a finite temperature and a gas pressure. Therefore, it is necessary to consider the free energy of a molecule in vapor phase. In this study, we investigate the stabilization of the Se- or S-treated GaAs(111)B surface structures by considering the beam equivalent pressure of As and Se(S) in a growth temperature using the first-principles calculations within the density functional theory. The chemical potentials of molecules are derived from the partition functions for the translation, the rotation, and the vibrational motions.

In the phase diagram for the actual experiment condition, T=800K, the mixed Se/As terminated surface appears in the Se pressure of 10^{-15}-10^{-5} Torr, being consistent with the recent experiment [5]. Surprisingly, the Se-terminated surface also becomes stable as the Se pressure increases. We will discuss the stabilization mechanism of the chalcogen-treated GaAs surfaces.

[1]J. Fan, H. Oigawa and Y. Nannichi, Jpn. J. Appl. Phys. **27**, L2125 (1998).

[2]T. Scimeca, Y. Watanabe, R. Berrigan, and M. Oshima, Phys. Rev. B **46**, 10201 (1992).

[3]V. N. Bessolov and M.V. Lebedev, Semiconductors **32**, 11 (1998).

[4]M.D. Pashley, Phys. Rev. B **40**, 10481 (1989).

[5]A. Ohtake and Y. Sakuma, Cryst. Growth Des. **17**, 363 (2017).

[6]A. Ohtake, S. Goto and J. Nakamura, Sci. Rep. **8**, 1220 (2018).

11:00am **EM+2D+AP+NS+PS-TuM10 Combining 2D and 1D Atomic Scale Tailored Nanowire Surfaces for Novel Electronics and Photonics***, **Anders Mikkelsen**,* Lund University, Sweden **INVITED**

The III-V nanowire (NW) technology platform has reached a level of advancement that allows atomic scale control of crystal structure and surface morphology as well as flexible device integration. In particular, controlled axial stacking of Wurtzite (Wz) and Zincblende (Zb) crystal phases is uniquely possible in the NWs. We explore how this can be used to affect electronic, optical and surface chemistry with atomic scale precision opening up for 1D, 2D and 3D structures with designed local properties.

We have previously demonstrated atomically resolved Scanning Tunneling Microscopy/Spectroscopy (STM/S) on a wide variety of these III-V NWs and on operational NW devices[1-4]. We now use these methods for studying atomic scale crystal phase changes, the impact on local electronic properties and demonstrating full atomic resolution STM during device operation[5-7]. We explore the surface alloying of Sb into GaAs NWs with controlled axial stacking of Wz and Zb crystal phases[5] demonstrating a simple processing-free route to 1D and 2D compositional control at the monolayer level. Further we show how Bi can form unique 1D and 2D structures in particular on the unique Wz GaAs NW segments. Using 5K STM/S we measure local density of states of Zb crystal segments in Wz InAs NWs down to the smallest possible atomic scale crystal lattice change [6], which is effectively a small 2D material segment in a 1D structure. We find that the general Zb electronic structure is preserved locally in even the smallest segments and signatures of confined states in them.

Characterization to the atomic scale during electrical and optical operation is necesarry to understand and develop the functionality of structures as discussed above. We demonstrate a novel device platform allowing STM/S with atomic scale resolution across a III-V NW device simultaneously with full electrical operation and high temperature processing in reactive gases[7].Using 5-15 femtosecond laser pulses combined with PhotoEmission Electron Microscopy (PEEM) we explore local dynamic response of carriers in the 1D Wz and Zb crystal phases down to a few femtoseconds temporally and a few tens of nanometer spatially[8].

[1] E. Hilner et al., Nano Lett., 8 (2008) 3978; M. Hjort et al., ACS Nano 6 (2012) 9679

[2] M. Hjort et al., Nano Lett., 13 (2013) 4492; M. Hjort et al., ACS Nano, 8 (2014) 12346

[3] J.L. Webb, et al Nano Lett. 15 (2015) 4865

[4] O. Persson et al., Nano Lett. 15 (2015) 3684

[5] M. Hjort et al Nano Lett., 17 (2017) 3634

[6] J.V. Knutsson e tal ACS Nano, 11 (2017) 10519

[7] J.L. Webb et al, Sci. Rep. 7 (2017) 12790

[8] E. Mårsell et al, Nano Lett. 18 (2018) 907

11:40am **EM+2D+AP+NS+PS-TuM12 Nanoflower Decorated GaN and AlGaN/GaN based Catalyst-free CO Sensors***, **Monu Mishra**, G. Gupta,* National Physical Laboratory, India

III-Nitride semiconductors owing unique material properties have proven their potential in the detection of light, chemical, biomolecules and toxic/explosive gases. Despite of numerous advantages *viz.* biocompatibility, high temperature/frequency tolerance and harsh/adverse environmental condition sustainability, the use of expensive catalysts (e.g. platinum) and higher operation temperature (>250°C) for gas sensing has plagued the development of GaN based cost-effective sensing technology. Upto the best of our knowledge, literature lacks any scientific report on the development of catalyst-free CO sensors operating at room-temperature using GaN or AlGaN/GaN structures indicating the necessity of dedicated scientific attention in this area. Therefore, we report the fabrication of nanoflowers-decorated GaN and AlGaN/GaN heterostructure based catalyst-free CO sensors operating at lower (including room) temperature. Planar as well as nanostructured GaN & AlGaN/GaN thin films were employed for sensors fabrication which exhibited significant CO sensing associated with its superior surface and interface properties. For in-depth understanding, the obtained results were thoroughly analyzed and correlated to investigate the underlying science/phenomenon which revealed that CO sensing on GaN (and AlGaN/GaN) is governed by the chemical nature of ambient-oxidation induced amorphous oxide (O_2^-, O^{2-} orOH^- species) layer grown on the surface and acting as a donor/acceptor state. Besides, electron accumulation at AlGaN/GaN interface influenced the critical parameters like schottky barrier height, ideality factor etc. perturbed the effective carrier transport and ultimately the device performance. The study demonstrate that development of catalyst-free room temperature operating GaN based CO sensors is feasible using nanostructured surfaces, though further research is required for optimization of device performance.

12:00pm **EM+2D+AP+NS+PS-TuM13 Surface Transfer Doping of Diamond by Complex Metal Oxides for Power Electronics: A Combined Experimental and Simulation Study***, **Vihar Georgiev**, A.J. Moran, A. McGhee,* University of Glasgow, UK

Diamond has unique properties that make it an attractive wide band-gap material to produce future high-performance electronic devices. With a wide band-gap of 5.5eV, a thermal conductivity 5 times greater than 4H-SiC, a high breakdown field and high hole and electron carrier velocities, diamond is a clear stand out candidate for high frequency and high power devices. However, the lack of a suitable doping mechanism has hindered the application of diamond in electronic devices. Conventional substitutional doping techniques are limited as it is difficult to substitute atoms into the diamond crystal lattice.

Surface Transfer Doping (STD) gives the use of diamond for such applications more promise. For STD to occur there are typically two prerequisites: hydrogen terminated diamond (H-diamond) and an electron accepting material in intimate contact with the H-diamond surface. The

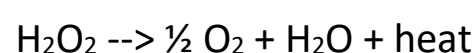

hydrogen termination gives the diamond a negative electron affinity which facilitates the transfer of electrons from the diamond to the electron-accepting material, creating a shallow, quasi two-dimensional hole gas (2DHG) in the diamond. This doping process traditionally relies upon interfacial electron transfer between the diamond valence band and favourable energy states provided by atmospheric molecules dissolved in a water layer naturally adsorbed on the diamond surface. However, the stability of this atmospheric layer, upon which the transfer doping process relies, has been a significant limiting factor in the production of high-power handling and robust operation devices.

One of the materials that can improve the performance and stability of STD in diamond are the metal oxides such as MoO_3 which acts as an alternative electron acceptor medium on the H-diamond surface. In order to validate and understand the physical and the chemical process in such STD, in this work we have combined experimental and simulation studies. The electrical characterisation is done by high temperature Hall measurements. Those experimental results are compared to numerical simulation based on the first principle methods such as Density Functional Theory. Comparing the simulation and experimental results revealed that the electrons are transferred from the diamond to the metal oxides, leading to formation of a sub-surface 2DHG in the diamond. Due to this transfer of electrons to the oxide the hole carrier concentration increases in comparison to the air-exposed H-diamond. Our work shows the potential to improve the stability and performance of hydrogen-terminated diamond electronics devices through incorporation of high electron affinity transition metal oxides.

Thin Films Division
Room A124-125 - Session TF+AP-TuM

ALD and CVD: Precursors and Process Development

Moderators: Paul Poodt, Holst Centre / TNO, The Netherlands, Erwin Kessels, Eindhoven University of Technology, The Netherlands

8:00am **TF+AP-TuM1 Mechanism-Based Precursor Design for CVD of Metal Oxides and Sulfides***, **Lisa McElwee-White,*** University of Florida **INVITED**

Aerosol-assisted chemical vapor deposition (AACVD) of WO_x was demonstrated using the oxo tungsten(VI) fluoroalkoxo single-source precursors, $WO[OC(CF_3)_2CH_3]_4$ (**1**) and $WO[OC(CH_3)_2CF_3]_4$ (**2**). Mechanistic studies of the decomposition of **1** and **2** were consistent with gas phase decomposition to yield tungsten (VI) dioxo intermediates during growth of WO_x materials. The dioxo tungsten alkoxide precursors $WO_2[OC(CF_3)_2CH_3](DME)$ (**3**) and $WO_2[OC(CF_3)_3](DME)$ (**4**) were then prepared as a means of independently generating intermediates involved in deposition of WO_x materials from **1** and **2**. Further experimental and computational mechanistic studies have led to synthesis of related precursors with other O-bound ligand types, including β-diketonates, β-ketoesterates, β-ketoiminates, and β-diketiminates, which have been used for deposition of WO_x films and nanostructures. Similar mechanism-based design strategies using S-bound ligands have been extended to precursors for deposition of MoS_2 and WS_2. Precursor syntheses, mechanistic studies, deposition of films under AACVD and CVD conditions, and characterization of the resulting materials will be discussed.

8:40am **TF+AP-TuM3 Improved Control of Atomic Scale Processing: Characterization and Optimization of Precursor Mass Delivery Utilizing a Novel Thermal Sensor***, **Daniel Alvarez**, J. Spiegelman, C. Ramos, Z. Shamsi,* RASIRC

ALD precursor utilization is a long-standing problem in semiconductor manufacturing. In general, precursors are quite expensive ($5-$25/gram), particularly where utilization is estimated as low as 5-10%. Thus far, chip manufacturers have been burdened by precursor costs and low wafer throughput. A non-optimized process consumes excess material and requires longer purge time.

For Area Selective Deposition (ASD), control of precursor mass delivery is even more critical to process viability. Here, excessive precursor material can initiate growth on "Non-growth" surfaces, leading to a need for intermittent etch steps.

More process control may make problematic processes viable for semiconductor manufacturing. Recently RASIRC introduced a novel dry hydrogen peroxide (H_2O_2) precursor. A novel H_2O_2 mass flow sensor was developed to aid in product characterization. This thermal sensor accurately measures heat of decomposition for minute amounts of H_2O_2:

H_2O_2 --> ½ O_2 + H_2O + heat

Our work uses this device to characterize H_2O_2 delivery parameters to:

1. Minimize total precursor mass required
2. Maximize precursor mass delivered in shortest time
3. Limit purge time for increased throughput
4. Minimize nucleation of "Non-growth" surfaces

Quantitative experimental methods are used to understand the effects of:

1. Ampoule headspace pressure
2. Carrier gas flow rate
3. Liquid precursor temperature
4. Precursor pulse time
5. Saturation efficiency of carrier gas with precursor vapor
6. Binary interactions for multicomponent liquids
7. System heat transfer
8. Ampoule design

An ALD simulation manifold was built to re-create typical ALD conditions. An automated test program controls valves and sensors to simulate process recipes. Initial results indicate highly variable mass delivery w.r.t. pressure. An ampoule outlet pressure of 20 torr results in 33.22 mg/min H_2O_2 mass delivery, vs 15.11 mg/min at 70 torr and 1.22 mg/min at 760 torr. Results are less affected by flow rate, where 0.5 slm at 22 torr leads to 33mg/min H_2O_2 vs 1.0 slm at 34 torr leads to 42 mg/min, and 2.0 slm at 57 torr leads to 44 mg/min. Here, increased mass delivery from higher flow rate is offset by a corresponding increase in pressure. In addition, while increased flow rate does not result in significant mass delivery increase for 2 slm, there is a significant decrease in precursor concentration, where the molar ratio of H_2O_2/N_2 is decreased by 70% vs 0.5 slm. Concentration effects are significant to film uniformity in ALD and have ramifications in ASD.

Mass delivery vs pulse time was also examined. Data will be presented for 3s, 1s, 0.3 sec, and 0.1s pulses. Application to process optimization will also be discussed.

9:00am **TF+AP-TuM4 Effect of Co-Reactant on the Atomic Layer Deposition of Copper Oxide***, **Jason Avila**, N. Nepal, V.D. Wheeler,* U.S. Naval Research Laboratory

Atomic layer deposition (ALD) of copper oxide presents a powerful opportunity to grow p-type semiconductor material for a wide variety of applications such as transparent conducting oxide, solar fuels catalysis, and power devices. There are, however, very few ALD processes to facilitate the growth of copper oxide. Cu(II) bis(dmiethylamino-2-propoxide) (Cudmap) has previously been used to grow copper metal using a reducing source such as tertiary butyl hydrazine.[1,2] Cudmap has also been demonstrated to grow Cu_2O using water as a co-reactant, self-reducing from Cu(II) to Cu(I) in the presence of water.[3] This study will examine the effect of ALD co-reactants, ozone and water, on the copper oxidation state of copper oxide films grown using Cudmap.

Copper oxide films were grown in a Veeco Savannah ALD reactor using Cudmap and ozone or water at 150 °C on Si and c-plane sapphire. This is the first experimental demonstration of CuO films using Cudmap and ozone. Using ozone, a growth rate of 0.18 Å/cycle was achieved at 150 °C, far higher than the measured growth rate of 0.04 Å/cycle when using water. Since growth rates are still quite slow, a vapor assisted precursor delivery system for the Cudmap was implemented and its ability to achieve higher growth rates will be presented.

XPS was able to confirm the presence of only the Cu(II) oxidation state with a Cu/O ratio of 1, verifying the deposition of CuO films. For comparison, films grown with water show the presence of only Cu(I) oxidation state and have a nearly stoichiometric with a Cu/O ratio of 2:1, confirming the deposition of Cu_2O films. AFM also indicated uniform, continuous film growth, independent of co-reactant, for films as thin as 2 nm. However, for a similar thickness, CuO films deposited with ozone were rougher than Cu_2O films grown with water. In addition to these initial results, comparison of the optical and electrical properties of the different copper oxide films for p-type semiconductor applications will be presented.

References

(1) Väyrynen, K.; Mizohata, K.; Räisänen, J.; Peeters, D.; Devi, A.; Ritala, M.; Leskelä, M. Chemistry of Materials 2017, 29, 6502.

(2) Kalutarage, L. C.; Clendenning, S. B.; Winter, C. H. Chemistry of Materials 2014, 26, 3731.

(3) Avila, J. R.; Peters, A. W.; Li, Z.; Ortuno, M. A.; Martinson, a. B. F.; Cramer, C. J.; Hupp, J. T.; Farha, O. Dalton Transactions 2017, 46, 5790.

9:20am **TF+AP-TuM5 Electron Enhanced Atomic Layer Deposition (EE-ALD) of Cobalt Films and Development of New Hollow Cathode Plasma Electron Source***, **Zachary Sobell,*** CU Boulder*; A.S. Cavanagh, S.M. George,* University of Colorado at Boulder

Cobalt films were grown with electron enhanced atomic layer deposition (EE-ALD) at room temperature using sequential surface reactions. The Co film growth was performed using sequential cobalt tricarbonyl nitrosyl (CTN, $Co(CO)_3NO$) exposures and low energy (75-175 eV) electrons. A hot filament electron flood gun was used as the electron source. The electrons desorb the CO and NO ligands from CTN on the surface and produce active sites for additional CTN adsorption. The maximum growth rate was 0.5 Å per cycle at an electron energy of 125 eV. Cobalt is important as an advanced interconnect material to replace copper or tungsten. Because the electron flux is normal to the substrate, Co EE-ALD may be used to facilitate bottom-up-fill of trenches and vias.

One difficulty with Co EE-ALD using the electron flood gun is the long cycle times of 540 seconds. Much of this cycle time is consumed protecting the flood gun filament from precursor exposures and the long duration of the electron exposure due to the limited current of the gun. 42% of the cycle time is needed for the warm up and cool down of the filament of the electron flood gun between CTN exposures. Another 44% of the cycle time is required for the electron exposures. An additional 14% of the cycle time is needed to reduce the precursor pressure in the chamber following CTN exposures. The cycle time could be reduced significantly using a more robust and higher flux electron source.

A new hollow cathode plasma electron source (HC-PES) has been developed to reduce the cycle time during EE-ALD. The HC-PES has a >100X increase in electron flux compared with the electron flood gun. The HC-PES also eliminates the warm-up and cool-down time of the filament of the electron flood gun. The electron current from the HC-PES can be switched from nanoamps to miliamps in < 10 ms. The HC-PES is also chemically insensitive and reduces the need for pumping out the chamber following CTN exposures. This presentation will report on the characterization of this new HC-PES and its use for Co EE-ALD.

9:40am **TF+AP-TuM6 Surface Science Studies of GaN Substrates Subjected to Plasma-Assisted Atomic Level Processes***, **Samantha G. Rosenberg,*** American Society for Engineering Education (residing at U.S. Naval Research Laboratory)*; D.J. Pennachio, E.C. Young, Y.H. Chang, H.S. Inbar,* University of California at Santa Barbara*; J.M. Woodward,* U.S. Naval Research Laboratory*; Z.R. Robinson,* SUNY Brockport*; J. Grzeskowiak,* University at Albany - SUNY*; C.A. Ventrice, Jr.,* SUNY Polytechnic Institute*; C.J. Palmstrøm,* University of California at Santa Barbara*; C.R. Eddy, Jr.,* U.S. Naval Research Laboratory

III-N semiconductors are well suited for applications in several important technological areas, including high current, normally-off power switches.[1,2] Such devices require heterostructures not readily achievable by conventional growth methods. Therefore, we have developed a technique adapted from atomic layer deposition (ALD), called plasma-assisted atomic layer epitaxy (ALEp).[2] Using surface science techniques, we strive to develop not only a fundamental understanding of the ALEp growth process but also complimentary atomic level processes (ALPs) that will result in the best preparation method for a pristine GaN starting surface for ALEp.

Here we employ *in-situ* and *in-vacuo* surface science studies of GaN substrate preparation to advance fundamental understanding of the ALEp process. Having optimized our GaN surface preparation (gallium flash off ALP),[3] we conduct *in-vacuo* X-ray photoelectron spectroscopy (XPS), reflection high-energy electron diffraction (RHEED), and scanning tunneling microscopy (STM) studies in the Palmstrøm Lab at UCSB to further refine both our process and our understanding. Preliminary XPS results show that a GFO ALP conducted at 250°C for 12 cycles reduces the oxygen content by 5% but shows no reduction in the carbon content, while a GFO ALP conducted at 400°C for 30 cycles reduces the carbon content by 60% but shows no reduction in the oxygen content. Other XPS results show that our previously reported optimal GFO ALP results in a ~25% reduction of carbon, while a similar 25% reduction of oxygen was achieved using a GFO ALP with or without TMG. We have also conducted comparable temperature program desorption (TPD) and low energy electron diffraction (LEED) experiments at SUNY Polytechnic Institute to correlate structural and chemical changes that occur on GaN surfaces treated with our GFO ALP. TPD shows that NH_3 is released from GaN surfaces not subjected to GFO ALP as it is heated past 150°C, while GFO ALP GaN surfaces show no NH_3 release upon subsequent TPD experiments. Both GaN surfaces, before and after TPD, show an unreconstructed 1x1 diffraction pattern in LEED.

1. N. Nepal, et al., Appl. Phys. Lett. 103, 082110 (2013)

2. C. R. Eddy, Jr, et al., J. Vac. Sci. Technol. A 31(5), 058501 (2013)

3. S. Rosenberg, et. al., J. Vac. Sci. Technol. A 37, 020908 (2019)

11:00am **TF+AP-TuM10 Reaction Pathways in Photolytic CVD of Platinum on Organic Thin Films***, **Bryan G. Salazar,*** University of Texas at Dallas*; H. Liu, L. McElwee-White,* University of Florida*; A.V. Walker,* University of Texas at Dallas

Chemical vapor deposition (CVD) is widely used to deposit materials including metals, oxides, and sulfides. However, CVD is generally unsuitable for use on organic substrates because it often requires high temperatures (> 200 °C). In this work we investigate photolysis as an alternative to thermal activation for CVD of metals on organic thin films. To study the role of precursor chemistry on the Pt CVD process we use three different precursors: $(COD)Pt(CH_3)_2$, $(COD)PtCl(CH_3)$, and $(COD)PtCl_2$. We also investigate the role of substrate functionality on the CVD process using three different self-assembled monolayers (SAMs) with carboxylic acid-, hydroxyl-, and methyl- terminal groups to model organic thin films. Solution-phase photochemistry studies and residual gas analysis indicate that the photolytic activation of $(COD)Pt(CH_3)_2$ and $(COD)PtCl(CH_3)$ occurs via the loss of a methyl radical, while the $(COD)PtCl_2$ occurs via the loss of a chlorine. Subsequently these radicals abstract ligands from the gas phase precursor and the organic surface leading to the formation of methane, chloromethane, chlorine and ethane. Using X-ray photoelectron spectroscopy and time-of-flight secondary ion mass spectrometry (TOF SIMS), we also investigated the reaction pathways involved on the organic surfaces. The data indicates that the deposition is highly dependent on the wavelength of light, the Pt precursor, and the SAM terminal group. Using $(COD)Pt(CH_3)_2$, we observe a small amount of Pt deposition on –OH and –COOH terminated SAM surfaces. In TOF SIMS we observe Pt- and O-containing ions indicating that Pt has inserted into the terminal group. Little, or no, deposition is observed on the $–CH_3$ terminated SAMs. In agreement with previous studies, the data also shows that the neutral polyhapto ligand, COD, is difficult to remove; there are Pt- and COD-containing species present on the surface. Further, the data indicates that there is some SAM decomposition during the deposition. In contrast, for $(COD)PtCl(CH_3)$ and $(COD)PtCl_2$ little, or no, Pt deposition is observed and the data indicates that the SAM layers decompose to form polyaromatic hydrocarbons. The damage appears to be caused by the formation of chlorine radicals during the photolysis, which can penetrate through and react with the SAM. In contrast, the methyl radical is larger leading to less SAM damage because it cannot penetrate through the SAM layer. These studies provide insight into the reaction pathways involved in photolytic CVD and the role of radicals in the subsequent deposition and interaction with organic layers. Such studies therefore aid in the rational design of photolytic CVD on organic substrates.

11:20am **TF+AP-TuM11 Process Development and Mechanism Analysis of Low Temperature ALD TiN with $TiCl_4$/Monomethylhydrazine***, **Taiki Kato,*** *Z. Ni, M. Matsukuma, H. Nakamura, Y. Ideno, Y. Serizawa,* Tokyo Electron Technology Solutions Limited, Japan

TiN is an important barrier metal for semiconductor devices. Nevertheless, it is difficult to form low-electrical-resistance TiN films at low temperature with existing thermal $TiCl_4/NH_3$ ALD processes. To overcome this difficulty, we tried a new azotizing gas MMH (Monomethylhydrazine: CH_3NHNH_2) instead of NH_3 and achieved low electrical resistance TiN (~1 mW.cm) under 300 deg C deposition temperature. XPS and AFM observations revealed that the film deposited with $TiCl_4$/MMH has smaller Cl concentration and is smoother than the one deposited with $TiCl_4/NH_3$. In this study, we analyzed the $TiCl_4$/MMH ALD reactions to clarify the process improvement mechanism when using MMH. Furthermore, we also analyzed the reactivity of $TiCl_4$ with NH_3 and with novel azotizing gases HZ (Hydrazine: H_2NNH_2) and UDMH (Unsymmetrical dimethylhydrazine: $(CH_3)_2NNH_2$) for future process development.

To analyze surface azotizing reactions, we used density functional theory calculation software, $DMol^3$. Surface reaction analysis of $TiCl_2$ termination revealed that the azotizing reactions removed Cl from the substrate by HCl gas generation and MMH was more reactive as an azotizing gas than NH_3. These results explained the experimental phenomenon in which MMH can remove Cl from a TiN film more efficiently than NH_3 and improve the film's roughness and electrical resistance. HZ and UDMH are also more reactive than NH_3 and are candidates for future azotizing gases.

Next, we analyzed gas phase decomposition reactivity of these agents for clarification of ALD process windows. This analysis is conducted by GRRM (Global Reaction Route Mapping) program which can search for reaction

paths automatically. Gas decomposition reaction paths search revealed that ALD processes of $TiCl_4$ / HZ, MMH and UDMH are feasible under 400 deg C.

Furthermore, we analyzed azotizing gas chain reactivity for safe conservation estimation. This analysis is calculated by a molecular dynamics simulator, ADF ReaxFF. We inspected the chain reactivity of HZ, MMH, and UDMH densely packed in a tight container at high temperature. Reaction MD simulations showed that UDMH is the safest, followed by MMH then HZ.

In summary, we developed a new thermal TiN ALD process with $TiCl_4$/MMH instead of existing NH_3. Our simulation studies suggest that MMH, HZ and UDMH can remove Cl from TiN film more efficiently than NH_3 and improve the film roughness and the electrical resistance. Other reaction paths analyses show that the novel azotizing agents also have ALD temperature process windows under 400 degC and that the safe conservation trend HZ < MMH < UDMH. These hydrazine-like agents are promising azotizing precursors for low temperature ALD.

11:40am **TF+AP-TuM12 Atomic Layer Deposition of Aluminum, Hafnium and Zirconium Oxyfluoride Films with Tunable Stoichiometry**, ***Neha Mahuli**, J.M. Wallas, S.M. George,* University of Colorado at Boulder

Metal oxyfluoride films are chemically robust and resistant to plasma corrosion. This study explored the atomic layer deposition (ALD) of various metal oxyfluorides including aluminum oxyfluoride (AlO_xF_y), hafnium oxyfluoride (HfO_xF_y) and zirconium oxyfluoride (ZrO_xF_y). Different deposition techniques were developed to obtain tunable stoichiometry of these metal oxyfluoride films. The complicating factor was fluorine/oxygen exchange and the diffusion of fluorine in the oxyfluoride film.

For the metal oxyfluoride deposition, H_2O and HF were used as the oxygen and fluorine sources. $Al(CH_3)_3$ was used as the Al source. Hf and Zr alkylamide precursors were used as the Hf and Zr sources. The metal oxyfluorides were deposited using either (1) the halide-exchange method or (2) the nanolaminate method. These two methods gave rise to tunable stoichiometry from pristine metal oxide to adjustable oxyfluoride to pristine metal fluoride.Both methods were evaluated using *in situ* quartz crystal microbalance (QCM) measurements and *ex situ* X-ray photoelectron spectroscopy (XPS) analysis.

The halide-exchange method is based on the facile exchange of oxygen by fluorine from HFbased on following equation (MO_x + yHFàMF_y + xH_2O). HF exposures after deposition of the metal oxide easily replaced oxygen with fluorine. The fluorine also diffused into the underlying metal oxide film as a function of time and temperature. The compositional control is achieved either using metal oxide layers of various thicknesses or different HF pressures. The rate of fluorine diffusion determined by *in-situ* QCM as well as *ex-situ* XPS was assigned as AlO_xF_y>ZrO_xF_y>HfO_xF_y.

The stoichiometry was also tuned using the nanolaminate method with different numbers of metal oxide ALD and metal fluoride ALD cycles. One supercycle (of ratio n:m) here consists of 'n' layers of metal oxide followed by 'm' layers of metal fluoride. The F:O ratios in the metal oxyfluoride films using this mechanism could be controlled over the full range of compositional ratios. The rate of fluorine diffusion in these systems was also found to be AlO_xF_y>ZrO_xF_y>HfO_xF_y.

12:00pm **TF+AP-TuM13 ALD on Thermally and Chemically Treated Fused Silica and Glass Surfaces**, ***Tahereh Gholian Avval**, G. Hodges, V. Carver, M.R. Linford,* Brigham Young University

Silanol (SiOH) and surface hydroxyl (OH) groups strongly affect the absorption behavior of species onto silica (SiO_2) surfaces. The density of hydroxyl (OH) groups on these surfaces are important for initiating and producing conformal thin films by atomic layer deposition (ALD). The combination of chemical and thermal treatments of surfaces in ALD increases insight into their chemistry. Different chemical treatments, including cleaning solutions of industrial importance, affect surface silanol density and consequently subsequent thin film growth by ALD. In this work, we describe the density of hydroxyl (OH) groups on fused silica surfaces and their effect on ALD. In particular, we hydroxylated pieces of fused silica with hydrofluoric acid (HF) and then heat treated it at 200, 500, 700 and 900 °C. The samples then underwent different numbers of ALD cycles to produce thin films of Al_2O_3. As expected, analysis of these surfaces by X-ray photoelectron spectroscopy (XPS) showed that higher temperatures lead to lower aluminum loading/deposition. As a result, heat-treated samples at 900 °C appear to be significantly depleted in surface silanols and lagged behind in thickness compared to the other samples. Other chemical treatments of industrial relevance for silica and glass were also considered in this study, including hydrochloric acid (HCl), tetramethylammonium hydroxide (TMAH), and a detergent. This information is important for ALD deposition of this important material.

Atomic Scale Processing Focus Topic
Room B130 - Session AP+EL+MS+PS+SS+TF-TuA

Advancing Metrology and Characterization to enable Atomic Layer Processing

Moderators: Eric A. Joseph, IBM T.J. Watson Research Center, Jessica Kachian, Intel Corporation

2:20pm **AP+EL+MS+PS+SS+TF-TuA1 In Situ Ellipsometry Characterization Of Atomic Layer Processes: A Review***, **James Hilfiker**, G.K. Pribil, J. VanDerslice,* J.A. Woollam Co., Inc. **INVITED**

Atomic layer processes such as atomic layer deposition (ALD) and atomic layer etch (ALE) provide monolayer-level thin film deposition or etch. Spectroscopic ellipsometry (SE) is ideally suited for the characterization requirements of such very thin layers. In situ SE provides real-time feedback, which is invaluable for establishing new atomic layer processes. In situ SE characterization has been adopted by many researchers due to its versatility. SE measurements are sensitive to deposition or etch at the (sub)monolayer level. The real-time evolution of film thickness provides details on nucleation periods or delays, the growth or etch rates per cycle, and verifies the self-limiting nature of a process. Multiple experiments can be performed within a single run by modifying the process conditions, allowing quick qualification of deposition temperatures, chemical exposure times, plasma influences, and purge times. In this paper, we will review the areas where in situ SE has been applied to both atomic layer deposition and etch.

We will also discuss the applications of in situ SE that benefit from a broad wavelength range. SE is best known for determining film thickness and optical constants. This characterization can be accomplished for many types of materials – dielectrics, semiconductors, organics, and even metals – provided the layer remains semi-transparent. Other material properties affect the optical constants and can be determined via this relationship. In situ SE has been used to estimate the crystal structure, composition, and even conductivity of thin films. We will discuss the advantages and limitations of in situ SE, which in many ways has proven to be an ideal partner for atomic layer processes.

3:00pm **AP+EL+MS+PS+SS+TF-TuA3 Elucidating the Mechanisms for Atomic Layer Growth through In Situ Studies***, **Jeffrey Elam**,* Argonne National Laboratory **INVITED**

Atomic Layer Deposition (ALD) provides exquisite control over film thickness and composition and yields excellent conformality over large areas and within nanostructures. These desirable attributes derive from self-limiting surface chemistry, and can disappear if the self-limitation is removed. Understanding the surface chemical reactions, i.e. the ALD mechanism, can provide insight into the limits of self-limitation allowing better control, successful scale up, and the invention of new processes. In situ measurements are very effective for elucidating ALD growth mechanisms. In this presentation, I will describe our recent investigations into the growth mechanisms of ALD nanocomposite films comprised of conducting (e.g. W, Mo and Re) and insulating (e.g. Al_2O_3, ZrO_2 and TiO_2) components using in situ measurements. These ALD nanocomposites have applications in particle detection, energy storage, and solar power. We have performed extensive in situ studies using quartz crystal microbalance (QCM), quadrupole mass spectrometry (QMS), Fourier transform infrared (FTIR) absorption spectroscopy, and current-voltage measurements. These measurements reveal unusual ALD chemistry occurring upon transitioning between the ALD processes for the two components. This results in unique reaction products that affect the properties of the films in beneficial ways. The knowledge gained from our in situ studies of the ALD nanocomposite films has helped us to solve problems encountered when we scaled up the ALD processes to large area substrates.

4:20pm **AP+EL+MS+PS+SS+TF-TuA7 Surface, Interface, or Film: A Discussion of the Metrology of ALD Materials in Semiconductor Applications***, **G. Andrew Antonelli**, N. Keller,* Nanometrics **INVITED**

Atomic layer deposition, etching, and interface engineering are enabling technologies for semiconductor manufacturing. These processes have led to an explosion in the use of laboratory techniques such as transmission electron microscopy and the need to bring such instruments closer to or into the fab itself. However, there remains a need for in-line, non-destructive, non-contact metrology capable of quickly characterizing and monitoring these extremely thin films on test structures, on product, or in device as these data are the only meaningful method for monitoring of ultimate device performance. Indeed, in cases such as the use of selective deposition or etching, no test vehicle other than the ultimate product may be relevant. A variety of measurement techniques with a focus on x-ray and optical probes as applied to this class of problems will be reviewed. Examples will be provided on relevant logic such as the Gat-All-Around FET and memory devices such as 3D NAND.

5:00pm **AP+EL+MS+PS+SS+TF-TuA9 In Line and Ex Situ Metrology and Characterization to Enable Area Selective Deposition***, **Christophe Vallee**, M. Bonvalot, B. Pelissier, J-H. Tortai, S. David, S. belahcen, V. Pesce, M. Jaffal, A. Bsiesy,* LTM, Univ. Grenoble Alpes, CEA-LETI, France*; R. Gassilloud, N. Posseme,* CEA-LETI, France*; T. Grehl, P. Bruner,* IONTOF GmbH, Germany*; A. Uedono,* University of Tsukuba, Japan

Innovation in materials, architectures (3D), gap filling technologies, lithography and etch processes are mandatory at every node of CMOS or memory devices. These challenging integration issues can be facilitated by the use of an integration scheme currently being intensively investigated known as area selective deposition (ASD). Criteria for an adequate area selective deposition process are: growth only on specific regions, high throughput compatible with industrial demands, no so-called mushroom profiles into adjacent features as well as no nuclei defectivity on undesired sites. Several routes can be developed to achieve an ASD process with ALD. The one discussed here concerns the deposition/etch approach which takes benefit from an *in situ* etching step inserted in a standard ALD cycle [1]. By incorporation of anisotropic or isotropic etching steps in the ALD process, "surface" selective deposition, as well as topographically selective deposition (TSD) have been obtained [2, 3]. The major current shortcoming of this approach lies in the deep insight which is required regarding elementary atomic-scale reaction mechanisms. Indeed, in the case of an ALD/ALE Area Selective Deposition process, a highly precise control of etching and its selectivity at the atomic scale is needed. Controlling the nature and density of defects induced by etching or passivation steps and understanding their impact on the physical and electrical properties of selectively deposited films are of course also required. Moreover, in order to optimize these processes, an accurate understanding of the underlying reasons why passivation after a low number of ALD cycles, is no more effective. Thus, *in situ* as well as *ex situ* monitoring and metrology are mandatory.

In this presentation, we will discuss how to optimize and understand atomic-scale reaction mechanisms in an ALD/ALE ASD process using combined *in situ* or *ex situ* measurements, such as ellipsometry, XPS, XRR, LEIS, FIB-STEM, and positron annihilation. We will show that when crosslinked, these technics are very effective to perform atomic scale metrology and characterization. As an example, we will discuss F atom localization and density in selectively deposited oxides thanks to a F-based ALE chemistry incorporated in the ALD process. In the case of a topographically selective deposition (TSD) process attempts will be presented to understand ion/surface interactions when low energetic ions are extracted from the plasma of the PEALD reactor both during deposition and plasma-ALE steps.

[1] R. Vallat et al, JVSTA **35** (2017) 01B104

[2] R. Vallat et al, JVSTA **37** (2019) 020918

[3] A. Chacker et al, APL **114** (2019)

5:20pm **AP+EL+MS+PS+SS+TF-TuA10 Recent Progress in Thin Film Conformality Analysis with Microscopic Lateral High-aspect-ratio Test Structures***, **Riikka Puurunen**,* Aalto University, Finland **INVITED**

Conformal thin films which cover complex 3D shapes with a film of uniform properties (thickness, composition, etc.) are increasingly demanded applications such as semiconductor devices, microelectromechanical systems, energy conversion/storage and catalysis. Atomic layer deposition (ALD) and its counterpart atomic layer etching (ALE) [together known as atomic layer processing (ALP)], are increasing in usage largely thanks to their known conformal character.

A question that needs to be asked in the R&D of 3D applications using conformal ALD/ALE processes is: how conformal is conformal; is the conformality sufficient to meet the specs? In semicon industry, vertical vias and cross-sectional transmission electron microscopy (TEM) are standardly used for conformality analysis. Recently, microscopic lateral high-aspect-ratio (LHAR) test structures have been developed to improve the conformality analytics capabilities. LHAR structures e.g. enable detailed conformality analysis at arbitrarily high aspect ratios (e.g., >5000:1), where no film can coat the 3D structure fully, thereby exposing the saturation

profile characteristic for the process. This, in turn enables the kinetic analysis of the process and e.g. extraction of the sticking coefficients related to the growth reactions.

This invited talk will address recent progress related to the fabrication and the use of microscopic LHAR conformality test structures. After the breakthrough with the first prototypes (PillarHall LHAR1; Gao et al. 2015, Mattinen et al. 2016; reviewed in Cremers et al., 2019), third and fourth generation prototypes have been developed (PillarHall LHAR3 and LHAR4). This work will review the conformality analysis progress enabled by the microscopic LHAR structures and discuss the benefits and challenges of this approach. Recent published progress includes the conformality modelling by Ylilammi et al. (2018) and experimental extraction of sticking coefficient by Arts et al. (2019). In addition, several other ongoing conformality analysis cases will be presented.

References

Arts, Vandalon, Puurunen, Utriainen, Gao, Kessels, Knoops, J. Vac. Sci. Technol. A 37, 030908 (2019); https://doi.org/10.1116/1.5093620

Cremers, Puurunen, Dendooven, Appl. Phys. Rev. 6, 021302 (2019); https://doi.org/10.1063/1.5060967

Gao, Arpiainen, Puurunen, J. Vac. Sci. Technol. A 33, 010601 (2015); https://doi.org/10.1116/1.4903941

Mattinen, Hämäläinen, Gao, Jalkanen, Mizohata, Räisänen, Puurunen, Ritala, Leskelä, Langmuir, 32, 10559 (2016); http://doi.org/10.1021/acs.langmuir.6b03007

Ylilammi, Ylivaara, Puurunen, J. Appl. Phys. 123, 205301 (2018); https://doi.org/10.1063/1.5028178

6:00pm **AP+EL+MS+PS+SS+TF-TuA12** ***In operando*XPS Study on Atomic Layer Etching of Fe and Co Using $Cl_2$and Acetylacetone or Hexafluoroacetylacetone***, **Zijian Wang**, O. Melton, D. Angel, B. Yuan, R.L. Opila,* University of Delaware

Etching of transition metals is one of the major challenges in magnetoresistive random-access memory (MRAM) device fabrication. In this work, atomic layer etching of iron and cobalt surfaces with halogen and an organic molecule was studied. We successfully performed etching of Fe and Co thin films via forming volatile metal complexes at low temperature with cyclic sequential reactions of Cl_2 and acetylacetone (acac) or hexafluoroacetylacetone (hfac) . The etching reaction mechanism of acac and hfac reacting with Clorine-modified Fe and Co surfaces was investigated: the surface was first activated with Cl_2 gas, and subsequently, the top layer of chlorinated metal was removed by reaction with a diketone (acac/hfac). The extent of Cl_2 reaction determines the etching rate of the metal. At substrate temperatures lower than 135°C, acac could remove the chlorinated Fe metal layer from Fe surfaces, but not chlorinated Co from Co surfaces. *In-operando* x-ray photoelectron spectroscopy (XPS) and density functional theory (DFT) simulation shows that the reaction of acac or hfac with Chlorinated Fe or Co surfaces is likely following a complex reaction pathway instead of simple diketone substitution for the metal chloride. Diketone decomposition may play an important role in the etching process.

Atomic Scale Processing Focus Topic
Room B130 - Session AP+BI+PS+TF-WeM

Surface Reaction Analysis and Emerging Applications of Atomic Scale Processing

Moderator: Eric A. Joseph, IBM T.J. Watson Research Center

8:00am **AP+BI+PS+TF-WeM1 Open Spaces in Al_2O_3 Film Deposited on Widegap Semiconductors Probed by Monoenergetic Positron Beams***, **Akira Uedono**,* University of Tsukuba, Japan*; T. Nabatame,* NIMS, Japan*; W. Egger, T. Koschine,* Universität der Bundeswehr München, Germany*; C. Hugenschmidt, M. Dickmann,* Technische Universität München, Germany*; M. Sumiya,* NIMS, Japan*; S. Ishibashi,* AIST, Japan **INVITED**

Positron annihilation is a useful technique for characterizing vacancy-type defects in semiconductors, and it has been successfully used to detect defects in GaN. This technique is also useful for detecting open spaces in thin amorphous films deposited on semiconductor substrates. When a positron is implanted into condensed matter, it annihilates with an electron and emits two 511-keV gamma quanta. The energy distribution of the annihilation gamma rays is broadened by the momentum component of the annihilating electron-positron pair. A freely diffusing positron may be localized in a vacancy-type defect because of Coulomb repulsion from positively charged ion cores. Because the momentum distribution of the electrons in such defects differs from that of electrons in the bulk material, these defects can be detected by measuring the Doppler broadening spectra of the annihilation radiation. Because the electron density in open spaces or vacancy-type defects is lower than that in the bulk, the lifetime of positrons trapped by such regions is longer than that of positrons in the delocalized state. Thus, the measurement of the positron lifetime also provides information of open spaces and vacancies in solid. In the present work, open spaces and defects in the Al_2O_3(25 nm)/GaN structure were probed by using monoenergetic positron beams.

Al_2O_3 films were deposited on GaN by atomic layer deposition at 300ºC. Temperature treatment above 800°C leads to the introduction of vacancy-type defects in GaN due to outdiffusion of atoms from GaN into Al_2O_3. The width of the damaged region was determined to be 40-50 nm from the Al_2O_3/GaN interface, and some of the vacancies were identified to act as electron trapping centers. In the Al_2O_3 film before and after annealing treatment at 300-900ºC, open spaces with three different sizes were found to coexist. The density of medium-sized open spaces started to decrease above 800°C, which was associated with the interaction between GaN and Al_2O_3. Effects of the electron trapping/detrapping processes of interface states on the flat band voltage and the defects in GaN were also discussed.

The present research suggests that the interaction between amorphous Al_2O_3 and GaN introduces not only vacancy-type defects in GaN but also changes the matrix structure of Al_2O_3 film. We also revealed that the electron trapping/detrapping processes of interface charge states are influenced by the defects introduced in GaN.

8:40am **AP+BI+PS+TF-WeM3 Surface Reaction Analyses of Atomic-layer Etching by Controlled Beam Experiments***, **Kazuhiro Karahashi**, T. Ito, S. Hamaguchi,* Osaka University, Japan

In manufacturing of modern advanced semiconductor devices such magnetoresistive random-access memories (MRAMs), phase-change random-access memories (PRAMs), and three-dimensional integrated circuit (3D IC) devices, damage-free high-precision etching for various materials is an indispensable process technology. Halogenation of a surface layer combined with low-energy ion bombardment or ligand-exchange of organic molecules for the formation of metal complexes is a surface reaction that may be used for such highly selective etching processes with atomic-scale precision. A better understanding of surface reactions taking place during the etching process often allows one to control and optimize the process more effectively. In this study, we have developed a new surface-reaction analysis system with highly controlled beams of various species and examined surface reaction mechanisms of plasma-assisted or thermal atomic-layer etching (ALE) processes for silicon (Si), copper (Cu), and nickel (Ni) films. The beam experiment of this system offers an experimental “simulation” of actual ALE surface reactions. The system is equipped with differentially-pumped multiple beam sources that can irradiate the sample set in an ultra-high-vacuum (UHV) chamber with different types of beams, i.e., low-energy ions, thermal molecules, metastable radicals, and atomic/molecular clusters, independently. During the beam irradiation, scattered and desorbed species may be measured by a differentially pumped quadrupole mass spectrometer (QMS). Time-resolved measurements of QMS synchronized with pulsed beam irradiation facilitate detailed analysis of the beam-surface interactions. Chemical states of adsorbed species on the sample surface may be measured by X-ray photoelectron spectroscopy (XPS). In this presentation, we discuss the mechanisms of halogenated-layer formation on the Si, Cu, or Ni surfaces by their exposure to XeF2 or Cl2 gases and the removal mechanisms of halogenated species from the surface by low-energy ion irradiation or surface heating. Thermal desorption mechanisms of Cu or Ni by the metal-complex formation with organic molecules (such as diketones) from its oxidized surface are also discussed

9:00am **AP+BI+PS+TF-WeM4 Surface Reaction Analysis of Fluorine-based Reactive Ion Etching (RIE) and Atomic Layer Etching (ALE) by Molecular Dynamics (MD) Simulation***, **Erin Joy Tinacba**, M. Isobe, K. Karahashi, S. Hamaguchi,* Osaka University, Japan

Plasma etching has always been a useful process in semiconductor device fabrication. There are several ways of using plasma etching such as reactive ion etching (RIE), wherein the material surface is bombarded with energetic ions while it also exposed to chemically reactive radicals from the plasma. Because of the energy provided by bombarding ions and high chemical reactivity on the surface, the surface is etched even at a relatively low temperature due to the combination of physical and chemical sputtering effects. RIE is often suited to fast etching processes of high aspect ratio structures since it can provide high etching yields. Another application of plasma etching is plasma-assisted atomic layer etching (ALE), wherein chemical and sputtering effects of typical plasma etching are separated into two steps. In a typical ALE process, the first step is an adsorption step wherein chemically reactive molecules or radicals from a plasma are used to modify the material surface. The modified monolayer or a thin layer on the material surface is then etched during the subsequent desorption step (second step) where low-energy ions bombard the surface. The etching reaction stops when the modified layer is depleted. This cycle is repeated many times until the desired etched depth is reached. The ALE process might be slow but it can provide tight control in the etch variability for sub-10 nm technology applications.

In this paper, molecular dynamic (MD) simulation is used to understand the effects of ions and radicals of high fluorine (F) content on etching reactions of silicon (Si), silicon dioxide (SiO_2), and silicon nitride (Si_3N_4), which may be observed in RIE processes based on, e.g., SF_6, C_2F_6, or NF_3 plasmas. If such a plasma is used as a radical source and ion bombardment steps by inert gas ions are separated from the radical exposure steps, an ALE process may be performed with similar surface reactions. In typical RIE, a supply of a large amount of fluorine to the surface by increasing the flux of energetic ions containing multiple F atoms (such as SF_5^+, $C_2F_5^+$ and NF_2^+ ions) and/or by increasing a F radical flux to the surface results in high etch rates. It has been found that the etching rates by such highly fluorinated ions obtained from MD simulations are in good agreement with experimental observations and the deep fluorination of the surface accounts for their high etch rates. Although fluorine may be considered too corrosive to be used for ALE, we also analyzed by MD simulation an ALE process by fluorine-containing radicals such as NF2 and compared the results with experimental observations.

9:20am **AP+BI+PS+TF-WeM5 Analysis of Metal Surface during Atomic Layer Etching with Gas Cluster Ion Beam and Organic Acid***, **Noriaki Toyoda**, K. Uematsu,* University of Hyogo, Japan

Surface states of metal surface after atomic layer etchings (ALE) with gas cluster ion beam (GCIB) and organic acid were investigated using surface analysis tools (mainly X-ray photoelectron microscopy). In recent years, we have reported the usage of GCIB irradiation for the removal steps of ALE. Since GCIBs are aggregates of thousands of gas atoms or molecules, the energy/atoms or energy/molecules can be easily reduced to several eV even though the total energy of GCIB is several keV. This characteristic is beneficial for low-damage irradiation. In additions, since GCIBs induce dense energy deposition, the bombarded area experiences transient high-temperature and high-pressure conditions. As a result, chemical reactions are enhanced at low-temperature. These characteristics are suitable for the removal step in ALE.

In this study, we have investigated the surface state of metal (Ni, Cu) after ALE with GCIB and organic acid using in-situ XPS. Prior to GCIB irradiation, metal surfaces were cleaned by Ar ions. Then Ni or Cu surface were exposed to acetic acids or acetylacetones. The surface layer with adsorbed organic acid on metals were removed by subsequent GCIB irradiation. The difference of the surface states of metal between Ar and O_2-GCIB

irradiation are compared with in-situ XPS results. Etching mechanism by GCIB in the presence of the adsorbed organic acid will be discussed.

9:40am **AP+BI+PS+TF-WeM6 In-situ Characterization of Growth Kinetics of Piezoelectric Films Grown by Atomic Layer Deposition Utilizing an Ultra-high Purity Process Environment**, ***Nicholas Strnad***, General Technical Services, LLC; *D.M. Potrepka,* U.S. Army Research Laboratory; *N. O'Toole, G.B. Rayner,* Kurt J. Lesker Company; *J.S. Pulskamp,* U.S. Army Research Laboratory

Recently, $PbZr_xTi_{1-x}O_3$ (PZT) was grown by atomic layer deposition (ALD) in a piezoelectric film stack that was micro-machined into electrically actuated cantilever beams. [1] ALD PZT is a process technology that may drive 3D PiezoMEMS that utilizes piezoelectric films deposited on micro-machined sidewall structures. AlN is also a desirable piezoelectric for 3D PiezoMEMS but integration has been hampered by its sensitivity to reactive background gases resulting in oxygen contamination of several atomic percent and above. [2] Reactive background gases can also impact oxide films by skewing the non-uniformity and growth-per-cycle (GPC). Thus, individual reactor conditions play a significant role in both the growth kinetics, and resulting quality of thin films grown by ALD. To address both of these issues there exists the need for ultra-high purity (UHP) process capability. Here, we present how the transition from non-UHP to UHP process environment affects ALD AlN and the constituent oxide films in ALD PZT. The UHP process environment also enables the rapid characterization of the reaction kinetics of ALD processes by in-situ ellipsometry. The reaction kinetics of several constituent oxides for ALD PZT are presented based on empirical in-situ observations.

References

[1] Strnad, N.A. (2019) Atomic Layer Deposition of Lead Zirconate-Titanate and Other Lead-Based Perovskites (Doctoral Dissertation) https://doi.org/10.13016/8dqx-7pev

[2] Chen, Z. (2019) Thermal atomic layer deposition of aluminum nitride thin films from AlCl3 (Master's Dissertation)

11:00am **AP+BI+PS+TF-WeM10 Nanoscale Surface Modification of Medical Devices using Accelerated Neutral Atom Beam Technology**, ***Dmitry Shashkov***, *J. Khoury, B. Phok,* Exogenesis Corp. **INVITED**

Controlling surface properties of biomaterials is vital in improving the biocompatibility of devices by enhancing integration and reducing bacterial attachment. We use Accelerated Neutral Atom Beam (ANAB) technology, a low energy accelerated particle beam gaining acceptance as a tool for nanoscale surface modification of implantable medical devices. ANAB is created by acceleration of neutral argon atoms with very low energies under vacuum which bombard a material surface, modifying it to a shallow depth of 2-3 nm. This is a non-additive technology that results in modifications of surface topography, wettability, and chemistry. These modifications are understood to be important in cell-surface interactions on implantable medical devices. Similarly, ANAB could be used to modify surfaces of medical device coatings (small molecules and proteins)., creating a native drug elution barrier. In this study, we characterize the effects of ANAB on several materials including metals (Ti, CoCr) and polymers (PEEK, PP, PVC) and measure the differential ability of eukaryotic versus prokaryotic cell attachment on these modified surfaces. We also study the ability of ANAB to create an elution barrier on a drug coating without the use of binding polymers. We identified that eukaryotic cells including mesenchymal stem cells (MSC) and osteoblasts increase attachment and proliferation on treated surfaces as measured by MTS assay and cell visualization by microscopy. MTS assay shows that by day 14, control PEEK has 9,925±1,994 cells while ANAB-treated PEEK has 88,713±6,118 cells (n=3; $p<0.0014$). At the same time, we find that bacterial cells including *S.aureus* and *P.aeruginosa* have a decreased ability to bind on the ANAB-treated surface. This dichotomy of cellular attachment may be attributed to the nano-scale surface topography, favoring larger eukaryotic cells while inhibiting attachment of smaller bacterial pathogens. In studies focusing on drug elution, rapamycin was spray-coated on the surface of CoCr bare metal stents and either left as control or ANAB-treated the surface of the drug. These stents were then placed in a plasma elution assay for up to 7 days. We found that untreated stents eluted off most of the drug within 24 hours, and 100% of it by 48 hours post-elution. The ANAB-treated stents, however, showed a favorable elution profile slowly releasing the drug over the 7 day period. ANAB, therefore, has many possible uses in medical device technology in increasing integration, decreasing bacterial attachment and potentially biofilm formation, and, if desired, create an elution profile for a combination drug-device without the use of binding polymers.

11:40am **AP+BI+PS+TF-WeM12 Chemically Enhanced Patterning of Nickel for Next Generation EUV Mask**, ***Xia (Gary) Sang***, *E. Chen,* University of California, Los Angeles; *T. Tronic, C. Choi,* Intel Corporation; *J.P. Chang,* University of California, Los Angeles

The ever-increasing demand in high-precision pattern definition and high-fidelity pattern transfer in the IC manufacturing industry calls for continuous advancement in lithography technology. Extreme Ultra-Violet (EUV) lithography is being widely adopted for defining sub-10 nm nodes. Due to its ideal optical properties, Ni is under active research as the future absorbing layer material in EUV masks, the profile of which determines the quality of resulting lithographic patterns. Contemporary techniques for patterning Ni rely on noble ion beam milling, which leaves considerable amounts of re-deposition on feature sidewall. Finding chemically selective patterning technique is thus of critical importance. Due to the etch-resistant nature of Nickel, removal at an atomic level is enabled by chemical modification of the surface through plasma exposure and subsequent introduction of organic ligands. Plausible chemicals are first screened by thermodynamic assessments from available databases, experiments were then conducted to validate the theoretical predictions.

Both blanket and patterned Ni thin films were studied using this reaction scheme. Organic chemistries, such as acetic acid and formic acid were first investigated to determine the feasibility of metal-organic formation through direct exposure. The efficacy of acetic acid and formic acid etching chemistries were confirmed through solution-based studies on Ni, the formation of Ni(CH3COO)2 and Ni(HCOO)2 were confirmed through mass spectrometry. Nickel oxide formation and subsequent removal were confirmed by quantifying the change in the relative intensities of peaks of metallic Ni (852.6 eV) and oxidized Ni (853.7 eV) by X-Ray Photoelectron Spectroscopy (XPS).

The chemical reactivity difference between Ni0 and Ni2+ was quantified in the work to explore the attainable etch selectivity. Due to the decrease in radical concentration and flux, vapor phase etching of metallic Ni resulted in small thickness reduction (~ 0.4 nm/cycle). It is then tested that surface modification, particularly oxidation, is capable of promoting subsequent reactions by lowering reaction energy barrier through metal oxide formation. An oxygen plasma treatment is added prior to acid vapor exposure, and this cyclic approach results in a relatively linear etch rate of ~ 2 nm/cycle, which translates to a 50:1 etching selectivity of NiO over Ni. The same cyclic approach was then applied to patterned samples, post-etch sidewall angle of ~ 85° is measured, which closely conserves the initial feature profile (~ 87°).

12:00pm **AP+BI+PS+TF-WeM13 Surface Reactions of Low Energy Electrons and Ions with Organometallic Precursors and their Relevance to Charged Particle Deposition Processes**, ***Rachel Thorman***, Johns Hopkins University; *E. Bilgilisoy,* FAU Erlangen-Nürnberg, Germany; *S. Matsuda, L. McElwee-White,* University of Florida; *D. Fairbrother,* Johns Hopkins University

Focused electron beam induced deposition (FEBID) and focused ion beam induced deposition (FIBID) are nanofabrication techniques where beams of charged particles (electrons or ions) create metal-containing nanostructures by decomposing organometallic precursors in low pressure environments. Consequently, the interactions of electrons and ions with surface-bound organometallic precursors are fundamental processes in these deposition processes. Previously performed ultra-high vacuum (UHV) studies on low energy (below 100 eV) electron interactions with adsorbed precursors (e.g. $Pt(PF_3)_4$, $MeCpPtMe_3$, and $Co(CO)_3NO$) have revealed that electron-induced reactions of surface bound precursors occurs in two sequential steps: (1) an initial step characterized by precursor decomposition/deposition and partial ligand desorption followed by (2) decomposition of the residual ligands. However, a similar level of understanding does not exist for low energy ion interactions with organometallic precursors. In this presentation, I will show that a low temperature, UHV surface science approach can serve as a platform to study the reactions of both low energy electrons (500 eV) and low energy ions (<1kV Ar^+ ions) with organometallic precursors. Results from *in situ* X-ray photoelectron spectroscopy (XPS) and mass spectroscopy (MS) clearly show that low energy electron and ion-induced reactions of several surface-adsorbed species, including $(\eta^5\text{-}Cp)Fe(CO)_2Re(CO)_5$, $Ru(CO)_4I_2$, $Fe(CO)_5$, and $Co(CO)_3NO$, are markedly different. Similarly to electron-induced reactions, low-energy ion-induced reactions proceed in a two-step process with an initial decomposition step primarily characterized by ligand loss. However, ligand loss is typically must more extensive than is observed for electron-induced reactions; for example, in the case of $(\eta^5\text{-}Cp)Fe(CO)_2Re(CO)_5$ and $Fe(CO)_5$, all CO ligands desorb in this initial step. The second step in the ion induced reactions can be described as a regime

primarily characterized by physical sputtering. These contrasting results are discussed in the context of different deposition mechanisms proposed for FEBID and FIBID.

Atomic Scale Processing Focus Topic
Room B130 - Session AP+PS+TF-ThM

Thermal Atomic Layer Etching

Moderators: Eric A. Joseph, IBM T.J. Watson Research Center, Harutyun Melikyan, Micron Technology

8:00am **AP+PS+TF-ThM1 A Challenge for Selective Atomic Layer Etching of Non-volatile Materials Using Organometalic Complex**, ***Yoshihide Yamaguchi**, S. Fujisaki, K. Shinoda,* Hitachi, Japan*; H. Kobayashi, K. Kawamura, M. Izawa,* Hitachi High Technologies, Japan **INVITED**

Remarkable progress on atomic layer etching (ALE) for non-volatile materials has been made in recent years. The typical procedure for thermal ALE of non-volatile materials such as HfO_2 is cyclic repetitions of formation and desorption of the organometallic complex at a constant temperature [1]. The most significant problem in thermal ALE is formation of a volatile organometallic complex layer on the surface. The organometallic complex layer prevents diffusion of etching species into the deep at the formation step and must be easily removed at the desorption step. The thermal ALE of La_2O_3, however, is difficult to apply because the organo-lanthanum complexes are easily decomposed by mild heating (< 200 deg. C) and fail to prevent the diffusion. To solve this thermal instability, the authors have applied a thermal cycle ALE [2,3], which is a combination of a formation of the organo-lanthanum complex at a low temperature and a desorption of the complex at a high temperature. In this paper, several results of our challenge for thermal ALE of non-volatile materials using a selective organo-metallization reaction on the surface will be discussed. Some guiding principles for the organo-metallization reaction will also be explained.

A La_2O_3 thin-film sputtering deposited on a SiO_2/Si wafer was used as a sample. First, the La_2O_3 film was exposed to vapor mixture of a diketone and a stabilizer as the etchant gas at below 150 deg. C. Then the sample was annealed up to 250 deg. C. Temperature dependence in the procedure was also evaluated. After these consecutive processes, the sample was analyzed by scanning electron microscopy, X-ray photoelectron spectroscopy. Formation of the organo-lanthanum complex showed temperature dependent quasi-self-limiting characteristics. In the lower temperature range, the self-limiting characteristics enable precise control of the organo-lanthanum complex formation. In the higher temperature range, the continuous characteristics enable a higher etch amount per cycle with high selectivity. Several differences between chemistry with and without a stabilizer in the etching gas will be discussed. The high etching selectivity of La_2O_3 to HfO_2 was also demonstrated. From these findings, we conclude that practical ALE of La_2O_3 has been successfully demonstrated.

[1] Y. Lee et al., Journal of Vacuum Science & Technology A 36, 061504 (2018).

[2] K. Shinoda et al., J. Phys. D: Appl. Phys. 50, 194001 (2017).

[3] Y. Yamaguchi et al., ALE workshop TuM4 (2018).

8:40am **AP+PS+TF-ThM3 Characterization of Isotropic Thermal ALE of Oxide Films and Nanometer-Size Structures**, ***Andreas Fischer**, A. Routzahn, T.B. Lill,* Lam Research Corporation

In this work, we have characterized the reaction of aluminum oxide via the DMAC ligand exchange mechanism.

Fluorination studies of aluminum oxide were performed using NF_3, CF_4 or anhydrous HF, respectively. We also explored various methods of fluorination of the oxide surface such as thermal, in-situ or remote plasma, respectively, and found that a sufficient fluorine concentration could be obtained with either of the methods or reactants to enable atomic layer etching (ALE).

To understand reaction kinetics, we examined the interaction of aluminum fluoride (AlF_3) films with DMAC. We found that AlF_3 etched until it was completely consumed by DMAC. An analysis of its temperature-dependence allowed us to extract activation energies for the ligand exchange mechanism.

In a third part we demonstrated the utility of HF/DMAC reaction for isotropic ALE applied to nanometer-size metal oxide structures on wafers. Various metal oxides were etched and selectivities between oxides and potential mask materials were determined.

9:00am **AP+PS+TF-ThM4 Advanced Selective Chemical Dry Etch for Oxide and Si-based Material**, ***Li-Hung Chen**, T. Kato, K. Nakahata, K. Takeya,* Tokyo Electron Technology Solutions Limited, Japan

As device features continuously shrink with introducing complex structures and new materials in semiconductor manufacturing, extremely high selectivity for etch processes have become more and more important. High selective chemical dry etch is developed utilizing a separated damage-free chemical removal chamber and sublimation chamber. The required selectivity is realized by using various chemistries and quantum mechanics analysis.

Firstly, HF/NH3 chemistry is used for oxide etch with high selectivity to SiN, Si, metals and resist. On the other hand, HF mono chemistry can etch SiN with high selectivity to oxide and Si. Quantum mechanics analysis revealed that NH_3 combined with HF enhances the SiO_2 reaction because of its lower activation energy. However, HF mono chemistry enhances the SiN reaction because of its lower activation energy than the oxide reaction[1)]. Secondly, Gas A chemistry is introduced for etching low quality oxide with selectivity >50 to both high quality oxide and SiN. The reaction rate barrier determined by quantum mechanics shows that etch reactivity with ALD-oxide is higher than with Th-SiO2 and SiN in Gas A etch process. Furthermore, Si and SiGe etch are evaluated with different Gas B/C ratio. Etch amount of Si is increased with increasing Gas C flow which can reduce activation energy from quantum mechanics simulation. Moreover, SiGe etching amount is decreased with increasing Gas C flow. This means that selectivity between Si and SiGe can be precisely controlled by Gas flow ratio.

Various applications can be realized by utilizing chemical dry etch with specific chemistries. For oxide etch processes such as fin recess, air gap, hard mask removal and surface clean, HF/NH3 chemistry can be used to meet critical criteria such as oxide selectivity to Si, SiN, resist and metal. CIP HW is developed to enhance throughput with excellent etch selectivity and uniformity. Additionally, HF mono-gas (or F-containing treatment) can dope Fluorine (F) into oxide film which is confirmed by depth profile analysis of secondary ion mass spectrometry (SIMS), and F implantation is known for dielectric breakdown life time improvement[2)]. Also, Gas A can be utilized in Silica oxide removal process, which requires high selectivity between low quality and high quality oxide. Finally, Si mandrel removal and Si or SiGe nanowire fabrication is introduced by controlling gas flow ratio. Further discussion will be presented on AVS 66th.

Reference

[1] T. Kato, et al., AVS 65th Int. Symp. & Exhibit. (2018)

[2] Y. Mitani, et al., Proc. Of IEEE P93-98 (1999)

9:20am **AP+PS+TF-ThM5 Mechanisms of Thermal Atomic Layer Etching (ALE) of Metal by Deprotonation and Complex Formation of Hexafluoroacetylacetone (hfacH)**, ***Abdulrahman Basher**[1], I. Hamada,* Osaka University, Japan*; M. Krstic,* Karlsruhe Institute of Technology (KIT), Germany*; M. Isobe, T. Ito,* Osaka University, Japan*; K. Fink,* Karlsruhe Institute of Technology (KIT), Germany*; K. Karahashi, Y. Morikawa,* Osaka University, Japan*; W. Wenzel,* Karlsruhe Institute of Technology (KIT), Germany*; S. Hamaguchi,* Osaka University, Japan

Thermal atomic layer etching (ALE) may be used for precise and damageless etching of difficult-to-etch materials such as Ni, Co, NiFe, MgO, and CoFeB, which can be used as materials for magnetic tunnel junction (MTJ) stacks of magnetic random access memory (MRAM) devices. The goal of this study is to understand the mechanisms of surface chemical reactions during thermal ALE of metal in general with oxidation and exposure to organic molecules. As a model case, we consider a two-step thermal ALE process of nickel (Ni) with an oxidation step and a gas exposure step at an elevated substrate temperature [1]. In the latter step, hexafluoroacetylacetone (hfacH) $CF_3C(OH)=CHC(O)CF_3$ is used as a reactive gas. In the oxidation step, a thin layer of NiO is formed on the Ni film surface and, in the gas exposure step, only (part of) this NiO layer is removed and thus self-limiting etching of Ni is achieved. Our main question is why NiO is etched but Ni is not etched by hfacH. This mechanism is studied with first-principle simulation of interaction of hfacH with Ni and NiO surfaces.

First, we examined interaction of hfacH with a metallic Ni surface, using a simulation code STATE [2,3], which is based on density functional theory (DFT) with pseudo-potentials and a plane wave basis set. Computationally, a metal surface is better represented by a plane wave basis set in general.

[1] **Coburn & Winters Student Award Finalist**

It has been found in our simulation that, as an hfacH molecule approaches a metallic Ni surface with thermal velocity, it is more likely to be decompose and fragmented, rather than forming a hexafluoroacetylacetonate anion (hfac-) by deprotonation. This is consistent with earlier experimental observations [1,4]. The simulation clearly shows an energy threshold for deprotonation of hfacH with a metallic Ni surface.

Second, we examined interaction of enol hfacH with a NiO surface using a simulation code Turbomole [5], which is based on DFT but with Gaussian type orbitals. To better represent a NiO surface, we used the embedded cluster method (ECM) with Turbomole. It has been found that, as an hfacH molecule approaches a NiO surface, it is likely to deprotonate by transferring its hydrogen ion (H+) to an O atom of the NiO surface and the resulting hfac- tends to bond with a Ni atom of the surface because of the highly ionic nature of NiO, where Ni and O atoms are positively and negatively charged, respectively. In this way, volatile $Ni(hfac)_2$ and H_2O can be formed when hfacH molecules interact with a NiO surface. Reaction energies of such interactions have been evaluated from the simulations.

----

[1] T. Ito, et al., AVS 65th International Symposium & Exhibition (2018).

[2] Y. Morikawa, H. Ishii and K. Seki, Phys. Rev. B, **69**, 041403 (2004).

[3] I. Hamada, Physical Rev. B **89**, 121103 (2014).

[4] H. L. Nigg and R. I. Masel, J. Vac. Sci. Techol. A **17**,3477 (1999).

[5] R. Ahlrichs, M. Bär, M. Häser, H. Horn, C. Kölmel, Chem. Phys. Lett. **162**, 165 (1989).

9:40am **AP+PS+TF-ThM6 Thermal Atomic Layer Etching of Amorphous and Crystalline Al_2O_3 Films**, ***Jessica A. Murdzek**, S.M. George,* University of Colorado at Boulder

Thermal atomic layer etching (ALE) can be achieved with sequential, self-limiting surface reactions. One mechanism for thermal ALE is based on fluorination and ligand-exchange reactions. For metal oxide ALE, fluorination converts the metal oxide to a metal fluoride. The ligand-exchange reaction then removes the metal fluoride by forming volatile products. Previous studies have demonstrated the thermal ALE of amorphous Al_2O_3 films. However, no previous investigations have explored the differences between the thermal ALE of amorphous and crystalline Al_2O_3 films.

This study explored the thermal ALE of amorphous and crystalline Al_2O_3 films. HF or XeF_2 was used as the fluorination reactant. Dimethylaluminum chloride (DMAC) or trimethylaluminum (TMA) was employed as the metal precursor for ligand-exchange. The amorphous Al_2O_3 films had a much higher etch rate per cycle than the crystalline Al_2O_3 films. When using HF and TMA at 300 °C, the amorphous Al_2O_3 was removed at 0.78 Å/cycle, whereas the crystalline Al_2O_3 showed no significant thickness removal after 250 cycles (See Supplemental Figure 1). When using XeF_2 and TMA at 300 °C, the etch rate was 0.66 Å/cycle for the amorphous Al_2O_3 film. In comparison, ALE only removed up to 10 Å of the crystalline Al_2O_3 film. XeF_2 may be able to fluorinate the near surface region of the crystalline Al_2O_3 film easier than the crystalline bulk of the film.

The differences between amorphous and crystalline Al_2O_3 are sufficient to obtain selective thermal ALE of amorphous Al_2O_3 in the presence of crystalline Al_2O_3. The investigations also examined the effect of annealing temperature on the etch rate per cycle. Amorphous Al_2O_3 was etched at approximately the same etch rate until the crystallization of amorphous Al_2O_3 at >880 °C. The thermal ALE of crystalline films is important because amorphous films may not crystallize easily when they are too thin. Consequently, amorphous films may have to be grown thicker, crystallized, and then etched back to obtain the desired ultrathin crystalline film thickness.

11:00am **AP+PS+TF-ThM10 Thermal Atomic Layer Etching (ALE) of Germanium-Rich SiGe Films**, ***Aziz Abdulagatov**, S.M. George,* University of Colorado at Boulder

The thermal atomic layer etching (ALE) of germanium-rich SiGe was demonstrated using an oxidation and "conversion-etch" mechanism (See Supplemental Figure 1). In this process, the SiGe surface was oxidized to a SiGe oxide layer using O_2. The SiGe oxide layer was then converted to an Al_2O_3 layer using trimethylaluminum (TMA). The Al_2O_3 layer was fluorinated by HF to an AlF_3 layer prior to the removal of the AlF_3 layer by ligand-exchange using TMA. The thermal ALE of SiGe films will be important for the fabrication of advanced MOSFET devices.

This study explored the thermal ALE of germanium-rich $Si_{0.2}Ge_{0.8}$ films. *In situ* spectroscopic ellipsometry was employed to monitor the thickness of both the $Si_{0.2}Ge_{0.8}$ and the surface oxide layer during ALE. These studies showed that the $Si_{0.2}Ge_{0.8}$ film thickness decreased linearly with number of reaction cycles while the surface oxide thickness remained constant. Using an O_2-HF-TMA reaction sequence, the $Si_{0.2}Ge_{0.8}$ ALE etch rate was 0.57 Å/cycle at 290°C. This etch rate was obtained using optimal reactant pressures of 25, 0.2 and 0.4 Torr, and dose times of 1.5, 1 and 1 s, for O_2, HF and TMA, respectively.

The $Si_{0.2}Ge_{0.8}$ ALE etch rate was lower at lower temperatures. Using an O_2-HF-TMA reaction sequence, the $Si_{0.2}Ge_{0.8}$ etch rate was reduced from 0.57 Å/cycle at 290°C to 0.07 Å/cycle at 225°C. The order of the reactant sequence also affected the $Si_{0.2}Ge_{0.8}$ etch rate. Changing the reactant sequence from O_2-HF-TMA to O_2-TMA-HF reduced the $Si_{0.2}Ge_{0.8}$ etch rate from 0.57 to 0.45 Å/cycle at 290°C. $Si_{0.2}Ge_{0.8}$ could also be etched selectively in the presence of Si and Si_3N_4. The $Si_{0.2}Ge_{0.8}$ etch rate was >10 times faster than the etch rate for Si or Si_3N_4 at 290°C (See Supplemental Figure 2).

11:20am **AP+PS+TF-ThM11 Thermal Atomic Layer Etching of GaN and Ga_2O_3 Using Sequential Fluorination and Ligand-Exchange Reactions**, ***Nicholas Johnson**, Y. Lee, S.M. George,* University of Colorado at Boulder

Atomic layer etching (ALE) of GaN and Ga_2O_3 is important for the fabrication of power electronics devices. Thermal ALE of GaN and Ga_2O_3 was performed using sequential, self-limiting surface reactions. The thermal ALE was accomplished using fluorination and ligand-exchange reactions. XeF_2 and HF were used as the fluorination reactants. BCl_3 was the main metal precursor for ligand-exchange. Ga_2O_3 was also etched using $Al(CH_3)_3$, $AlCl(CH_3)_2$, $TiCl_4$ or $Ga(N(CH_3)_2)_3$ as the metal precursors for ligand-exchange.

Crystalline GaN samples prepared using MOCVD techniques at the US Naval Research Laboratory were etched with sequential XeF_2 and BCl_3 exposures. GaN etch rates varied from 0.18 to 0.72 Å/cycle at temperatures from 170 to 300°C, respectively (see Supplemental Figure 1). Because the GaN etch rates were self-limiting versus BCl_3 exposure and BCl_3 pressure, the GaN etching mechanism is believed to involve XeF_2 fluorination of GaN to GaF_3 and then ligand-exchange between BCl_3 and GaF_3 to yield volatile BCl_wF_x and GaF_yCl_z species. GaN fluorination using a NF_3 plasma was also successful for etching crystalline GaN at 250°C.

Ga_2O_3 samples deposited using ALD techniques were etched with sequential HF and BCl_3 exposures. Ga_2O_3 etch rates varied from 0.59 to 1.35 Å/cycle at temperatures from 150 to 200°C, respectively. The Ga_2O_3 etch rates were self-limiting versus HF and BCl_3 exposure. Ga_2O_3 ALE was also performed using HF for fluorination and a variety of metal precursors for ligand-exchange. Ga_2O_3 etch rates at 250°C were 0.2, 0.8, 1.1 and 1.2 Å/cycle for $Ga(N(CH_3)_2)_3$, $TiCl_4$, $Al(CH_3)_3$ and $AlCl(CH_3)_2$ as the metal precursors, respectively (see Supplemental Figure 2). The wide range of metal precursors that can etch Ga_2O_3 argues that the ligand-exchange reaction with GaF_3 is facile.

11:40am **AP+PS+TF-ThM12 Mechanistic Insights into Thermal Dry Atomic Layer Processing of Metals**, ***Andrew Teplyakov**,* University of Delaware **INVITED**

The mechanisms of thermally induced reactions of atomic layer deposition (ALD) and atomic layer etching (ALE) can be sometimes viewed as proceeding in opposite directions. However, for atomic layer processing of metals, that would mean that the best designed and most efficient reaction pathways leading to metal deposition would produce insurmountable energy barriers for a reverse process. If ligand detachment, exchange, and decomposition could be desirable for ALD, the etching of the same metals would require careful consideration of the etching mechanisms at the atomic and molecular level. Given that the mechanisms of ALE can be very complex, the key concepts and approaches will be described here for thermal dry etching processing, which would allow for eliminating the role of solvents and for distinguishing thermodynamic and kinetic regimes of etching. The mechanistic investigation of thermal dry etching of cobalt will be the primary target of this work. This process will be used to illustrate the limitations of the single-reagent etching by analyzing the reaction of 1,1,1,5,5,5-hexafluoro-2,4-pentanedione (hexafluoroacetylacetone, hfacH) or 2,4-pentanedione (acetylacetone, acacH)) with a clean cobalt surface. Then the effects of surface oxidation and chlorination will be explored as a means of kinetically controlled process. Finally, a number of potential effects of the mechanisms of dry etching on the morphology of the surfaces produced and, specifically, on the "smoothing" effect of dry etching will be discussed.

Surface Science Division
Room A220-221 - Session SS+2D+AP+AS+OX+SE-ThA

Dynamics at Surfaces/Reactions and Imaging of Oxide Surfaces

Moderators: Irene Groot, Leiden University, The Netherlands, William E. Kaden, University of Central Florida

2:20pm **SS+2D+AP+AS+OX+SE-ThA1 Adsorption, Reaction, and Diffusion of Energetic Reagents on Morphologically Diverse Thin Films***, **Rebecca Thompson**[12], M.R. Brann, S.J. Sibener,* The University of Chicago

I present work from two studies illustrating the impact of condensed-phase film morphology on reaction kinetics and surface adsorption. To begin, I will discuss the **oxidative reactivity of condensed propene films**. This work is conducted in a state-of-the-art ultra-high vacuum chamber equipped for operation at cryogenic substrate temperatures. Time-resolved reflection absorption infrared spectroscopy (RAIRS) is used to track propene reactivity when films are exposed to a supersonic expansion of ground state oxygen atoms, O(^{3}P). I demonstrate that propene reacts significantly on exposure, producing primarily propylene oxide and propanal. Oxide production is significant; partial oxidation products are rarely observed in gas phase studies and olefin oxides are incredibly important chemical intermediates in a variety of industrial processes. Regardless of initial film thickness, the reaction follows zero order kinetics, with a calculated activation energy of 0.5 kcal mol^{-1}. This low barrier closely matches that reported in gas phase studies, suggesting that the condensed-phase reaction is likely diffusion-limited. I also highlight that the propene deposition temperature has a substantial impact on reactivity. Films deposited below 50 K produce dramatically different RAIR spectra that correspond to a more amorphous film composition. These films are nearly unreactive with O(^{3}P), indicating that oxygen diffusion is directly tied to the density and ordering in the more crystalline film.

This dependence on film structure is also observed in the second study, which explores **embedding in and adsorption on crystalline, non-porous amorphous, and porous-amorphous water ice films**. Using a combination of supersonic molecular beams, RAIRS and King and Wells mass spectrometry techniques, I demonstrate that direct embedding into the bulk is remarkably insensitive to film structure; the momentum barrier is identical between amorphous and porous-amorphous ice films. Below this barrier, however, sticking probabilities differ considerably between the different films, suggesting that the pore structure is more efficient at dissipating incident energy. These discoveries are critical for the accurate quantitative modeling of molecular uptake and reactivity on icy astrophysical bodies such as comets and planetismals. When taken together, these two studies provide fundamental mechanistic insight into the sticking, diffusion, and reactivity of small molecules on complex films, with a specific emphasis on the impact of film morphology and organization.

2:40pm **SS+2D+AP+AS+OX+SE-ThA2 Oxidation of Semiconductors and Semimetals by Supersonic Beams of O_2 with Scanning Tunneling Microscopy Visualization***, **Ross Edel**[3], T. Grabnic, B. Wiggins, S.J. Sibener,* The University of Chicago

Our research examines the oxidation of semiconductor and semimetal surfaces using a novel, one-of-a-kind instrument that combines a supersonic molecular beam with an in-line scanning tunneling microscope (STM) in ultra-high vacuum. This new approach to surface reaction dynamics provides spatiotemporal information on surface oxidation over nanoscopic and mesoscopic length scales. We have uncovered the kinetic and morphological effects of oxidation conditions on three technologically relevant surfaces: Si(111)-7×7, highly oriented pyrolytic graphite (HOPG), and GaAs(110). A complete understanding of the oxidation mechanism of these surfaces is critical due to their technological applications and roles as model systems. Samples were exposed to O_2 with kinetic energies from 0.4-1.2 eV and impingement angles 0-45° from normal, with STM characterization between exposures. In some cases, we were able to monitor the evolution of specific features by revisiting the same nanoscopic locations. Our study of Si(111)-7×7 revealed two oxidation channels, leading to the formation of dark and bright reacted sites. The dark sites dominated the surface and exhibited almost no site selectivity while the bright sites preferred the corner sites of the 7×7 unit cell. Our observations suggest that two adsorption pathways, trapping-mediated and direct chemisorption, occur simultaneously. On HOPG, we found that different oxygen energies, incident angles, and surface temperatures produce morphologically distinct etching features: Anisotropic channels, circular pits, and hexagonal pits. Reaction probability increased with beam energy and demonstrated non-Arrhenius behavior with respect to surface temperature, peaking at around 1375 K. Finally, oxidation of GaAs(110) was found to proceed by two morphologically distinct, competing mechanisms: a homogeneous process leading to layer-by-layer oxide growth, and a heterogeneous process with oxide islands nucleating from surface defects. The rates of both mechanisms change with O_2 kinetic energy, with homogeneous oxidation dominating at lower energies (<0.7 eV) and heterogeneous oxidation with higher energies (≥1.0 eV). The results obtained in this work provide vital information about the morphological evolution and kinetics of semiconductor and semimetals, offering a comprehensive overview of the spatiotemporal correlations that govern oxidation dynamics on surfaces.

3:00pm **SS+2D+AP+AS+OX+SE-ThA3 Studying Molecule-Surface Interactions using Rotational Orientation Control of Ground-State Molecular Beams***, **Gil Alexandrowicz**,* Swansea University, UK **INVITED**

Performing quantum state selective experiments of molecule-surface collisions provides unique insight into the interaction potential. One particularly tricky molecular property to control and measure is the rotational projection states, i.e. the orientation of the rotational plane of the molecule. Previous data was mostly restricted to photo-excited/paramagnetic species. In this talk, I will describe the molecular beam apparatus which allows to control and measure the rotational orientation of ground state molecules [1], present new experimental results for H_2 colliding with ionic surfaces and discuss the future of this new technique in terms of studying molecule-surface interaction-potentials and modifying the outcome of reactive molecule-surface collisions.

[1] Nature Communications, 8, 15357 (2017).

4:00pm **SS+2D+AP+AS+OX+SE-ThA6 Diffusion of (100)-epitaxially Supported 3D fcc Nanoclusters: Complex Size-dependence on the Nanoscale***, **King Chun Lai**, J.W. Evans,* Iowa State University

Diffusion of supported 3D nanoclusters (NCs) followed by coalescence leads to coarsening of ensembles of supported NCs via Smoluchowski Ripening (SR) which is a key pathway for degradation of supported metal catalysts. The dependence of the NC diffusion coefficient, D_N, on size N (in atoms) is the key factor controlling SR kinetics, and traditional treatments assumed simple monotonic decrease with increasing size. We analyze a stochastic model for diffusion of (100)-epitaxially supported fcc NCs mediated by diffusion of atoms around the surface of the NC. Multiple barriers for surface diffusion across and between facets, along step edges, etc. are chosen to accurately describe Ag [Lai and Evans, Phy. Rev. Materials 3 (2019) 026001]. KMC simulations reveal a complex oscillatory variation of D_N with N. Local minima D_N sometimes but not always correspond to $N = N_c$ where the equilibrium Winterbottom NC structure is a closed-shell. Local maximum generally correspond to $N = N_c + 3$. The oscillatory behavior is expected to disappear for larger N above $O(10^2)$. Behavior has similarities to but also basic differences from that for 2D supported NCs [Lai et al Phys. Rev. B 96 (2017) 235406]. Through detailed analysis of the energetics of the 3D NC diffusion pathway (which involves dissolving and reforming facets), we can elucidate the above behavior as well as observed trends in effective diffusion barrier.

4:20pm **SS+2D+AP+AS+OX+SE-ThA7 Oxide Surface Formation on Rh Nanoparticle during O_2 Exposures Observed by Atom Probe Microscopy**, ***Sten Lambeets***, Pacific Northwest National Laboratory*; T. Visart de Bocarmé,* Université Libre de Bruxelles, Belgium*; N. Kruse,* Washington State University*; D.E. Perea,* Pacific Northwest National Laboratory

Metallic surfaces may undergo a series of surface and subsurface structural and chemical transformations while exposed to reactive gases that inevitably change the surface properties. Understanding such dynamics from a fundamental science point of view is an important requirement to build rational links between chemical/structural surface properties and design new catalysts with desired performance or new materials with enhanced resistance to corrosion. The research presented here addresses the early oxide formation dynamics on a rhodium (Rh) single nanoparticle during O_2 exposures and reveals the inter-facet cooperation between Rh{012} and Rh{113} facets, as well as the important role that the subsurface plays.

[1] **Morton S. Traum Award Finalist**
[2] **National Student Award Finalist**
[3] **National Student Award Finalist**

Field Ion and Field Emission Microscopies (FIM and FEM) enable correlative atomic to nanoscale imaging of the surface of a very sharp Rh needle, the apex size and shape of which models that of a Rh nanoparticle. FIM is used to map, with atomic lateral resolution, the Rh surface revealing a complex network of crystallographic facets, while FEM is used to observe and record O_2 dissociative adsorption and subsequent reaction with H_2 over this same surface of Rh in real-time with nano-scale lateral resolution. Since FEM imaging relies on local work function variations, it notably can be used to follow the fate of adsorbed oxygen atoms (O(ads)) on the Rh surface. As a result, we directly observe that the O_2 dissociative adsorption is mainly active on the Rh{012} regions. The application of Atom Probe Tomography (APT) provided a means to map the fate of the absorbed oxygen leading to bulk oxide formation through Rh{113} facets. Thus the correlative combination of FIM, FEM, and APT provides unique insight into the mechanism of bulk oxide formation starting from the dissociative oxygen absorption occurring at {012} facets and subsurface penetration of the adsorbed oxygen occurring through {113} facets. leading to a preferential accumulation of the oxygen within the bulk along the [111] direction. This work offers a unique methodology to explore the interactions between the different crystal facets of a complex surface, to explore the complex dynamics linking the surface and the bulk, and finally, offers exciting perspectives leading to a better understanding of heterogeneous catalysis and corrosion dynamics.

4:40pm **SS+2D+AP+AS+OX+SE-ThA8 Noncontact AFM on Oxide Surfaces: Challenges and Opportunities***, **Martin Setvin**,* TU Wien, Austria **INVITED**

Recent development of the noncontact atomic force microscopy (nc-AFM) has opened new possibilities in different fields – imaging of organic molecules [1], controlling the charge state of adsorbed species [2], or enhanced chemical resolution of surface atoms [3]. I will focus on the emerging possibilities and opportunities in the field of oxide surfaces and their surface chemistry.

The limits of atomic resolution will be illustrated on clean and water-exposed binary oxides like TiO_2, In_2O_3 or iron oxides. The enhanced chemical resolution of nc-AFM offers a unique opportunity for approaching complex materials with ternary chemical composition. This will be demonstrated on bulk-terminated perovskites $SrTiO_3$ and $KTaO_3$. A dedicated cleaving procedure [4,5] allows preparing flat regions terminated by domains of SrO/TiO_2 (or KO/TaO_2) with a well-defined atomic structure. The surface stability, point defects, electronic structure, and chemical properties of such surfaces will be discussed and linked to the incipient-ferroelectric character of these materials.

[1] Gross, L.; Mohn, F.; Moll, N.; Liljeroth, P.; Meyer, G., *Science* 2009, *325*, 1110

[2] Gross, L.; Mohn, F.; Liljeroth, P.; Repp, J.; Giessibl, F. J.; Meyer, G., *Science* **2009,***324*, 1428

[3] Sugimoto, Y.; Pou, P.; Abe, M.; Jelinek, P.; Perez, R.; Morita, S.; Custance, O., *Nature* **2007,***446*, 64

[4] I. Sokolovic, M. Schmid, U. Diebold, M. Setvin, *Phys. Rev. Materials* 3, 034407 (2019)

[5] M. Setvin, M. Reticcioli, F. Poelzleitner, J. Hulva, M. Schmid, L. A. Boatner, C. Franchini, U. Diebold, *Science* 359, 572-575 (2018)

5:20pm **SS+2D+AP+AS+OX+SE-ThA10 Edge-Enhanced Oxygen Evolution Reactivity at Au-Supported, Ultrathin Fe2O3 Electrocatalysts***, **Xingyi Deng**, D. Kauffman, D.C. Sorescu,* National Energy Technology Laboratory

Transition metal oxides have been emerging as promising candidates to replace the state-of-the-art IrO_2 electrocatalysts for oxygen evolution reaction (OER) in alkaline electrolyte, but their key structure-property relationships are often shadowed by heterogeneities in the typical catalyst samples. To circumvent this challenge, we have combined ultrahigh vacuum surface science techniques, electrochemical measurements, and density functional theory (DFT) to study the structure-dependent activity of well-defined OER electrocatalysts. We present direct evidence that the population of hydroxylated Fe edge-site atoms correlates with the OER activity of ultrathin Fe_2O_3 nanostructures (~0.5 nm apparent height) grown on Au(111) substrates, and the Fe_2O_3/Au catalysts with a high density of edge sites can outperform an ultrathin IrO_x/Au OER catalyst at moderate overpotentials. DFT calculations support the experimental results, showing more favorable OER at the edge sites along the Fe_2O_3/Au interface with lower predicted overpotentials resulted from beneficial modification of intermediate binding. Our study demonstrates how the combination of surface science, electrochemistry, and computational modeling can be used to identify key structure-property relationships in a well-defined electrocatalytic system .

Atomic Scale Processing Focus Topic
Room Union Station B - Session AP-ThP

Atomic Scale Processing Poster Session

AP-ThP1 Atomic Resolution Characterization of Atomic Layer Etching Normally-off AlGaN/GaN Hetrostructure Device by Using Aberration-corrected STEM, ***Chien-Nan Hsiao***, Taiwan Instrument Research Institute, National Applied Research Laboratories, Taiwan, Republic of China; *C.P. Lin, C.C. Chen, M.H. Chan, W.-C. Chen, F.Z. Chen,* National Applied Research Laboratories, Taiwan, Republic of China

An in-situ plasma enhanced atomic layer etching system has been design and fabricated. N_2O , BCl_3 and Ar plasma were used as the precursor for III-group epitaxy layer at various temperature. The optical detector was used to in-situ monitor the plasma spectrum during the step by step etching process. The AlGaN/GaN hetrostructure of normally-off high power GaN device (150 V) and etching per cycle of ALE were investigated using an aberration-corrected scanning transmission electron microscope with energy distribution spectrometer. It is found that the layer by layer etching feature shows the process is a controlled self-limited reaction. In addition, the influence of various aberration coefficients such as defocus, astigmatism, coma, spherical aberration and star aberration on the shape of the probe and more importantly on the electron intensity distribution within the probe was calculated. The accuracy required for compensation of the various aberration coefficients to achieve sub-angstrom resolution (0.078 nm) with the electron optics system was evaluated by the calculation of phase shift. Furthermore, the saturation curve of atomic etching rate and precursor pulsed time has been established. The etching per cycle of AlGaN is around 0.33 nm.

AP-ThP2 Programmable Radical-Assisted Sputtering Enabling Designed Deposition Processes with Atomic Layer Accuracy, ***Hideo Isshiki***, *Y. Tanaka,* The University of Electro-Communications, Japan; *S. Saisho,* Shincron Co. LTD., Japan

A programmable multi-cathode plasma generator (PMCPG), which consists of a high voltage DC power supply, a multichannel digital pattern generator (DPG), and a high voltage switch (HV-SW) attached to each cathode, was developed. We have applied PMCPG to radical-assisted sputtering (RAS) process, and called it "Programmable RAS (PRAS) ". The RAS system provided by Shincron has been widely used for mass production on the optical thin film coating of metal oxide compounds. RAS process is a process alternating metal ultra-thin layer deposition and radical reaction on the metal surface deposited just before. Conventional RAS system needs a large space to spatially separate above two steps. RAS process has a possibility to realize functional materials controlled with atomic layer accuracy. Therefore, the laboratory size RAS system is required to advance the development of functional material devices. We noticed that RAS process can be performed by switching between the metallic mode and the reactive mode found in reactive sputtering. So we have developed PMCPG to enable the time-separated RAS process.

DC pulse plasma on each cathode is generated by direct drive of DC power supply using DPG and the attached HV-SW, and a certain metal sputter is performed selectively under the metallic mode. On the other hand, radical source gasses are fed into the chamber synchronized with the plasma generation on the other cathode, generating the radicals. At the same time, the deposition rate decreases abruptly because of shift to the reactive mode with skipping over the hysteresis region. In this way, the radical reactions on a deposited metal surface proceed preferentially, and then RAS process is complete. The process cycle corresponding to a metal oxide monolayer was estimated to be a few seconds. We also confirmed that the plasma generation using the electronic switching system follows the pulse train more than 50kHz. From the fact that DPG can generate various pulse train for the plasma generation, it is suggested that PRAS enables designed deposition processes with atomic layer accuracy. In this work, YSZ and cubic $(Er_{0.1}Y_{0.9})_2Zr_2O_7$ were successfully synthesized by PRAS. Typical deposition rate of transparent YSZ was more than 1.5µm/hour, indicating the reproduction of RAS process. Layer-by-layer deposition of cubic $(Er_{0.1}Y_{0.9})_2Zr_2O_7$ was also confirmed through X-ray diffraction. This system has four cathodes and can meet the requirements for plasma generation on each cathode independently. We expect that PRAS system enables an artificial material synthesis driving “the materials informatics”.

You can find the demo of PMCPG at http://www.flex.es.uec.ac.jp/?page_id=243.

Author Index

Bold page numbers indicate presenter

— A —
Abdulagatov, A.I.: AP+PS+TF-ThM10, **20**
Abelson, J.R.: TF+2D+AP+EL+SS-MoA5, 7
Agarwal, S.: AP+2D+EM+PS+TF-MoM10, **2**; AP+2D+EM+PS+TF-MoM2, 1; AP+2D+EM+PS+TF-MoM8, 2
Akaishi, A.: 2D+AP+EM+MI+MN+NS+PS+TF-MoA9, 4
Alexandrowicz, G.: SS+2D+AP+AS+OX+SE-ThA3, **21**
Al-Mamun, M.S.: EM+2D+AP+NS+PS-TuM4, 9
Alvarez, D.: TF+AP-TuM3, **11**
Angel, D.: AP+EL+MS+PS+SS+TF-TuA12, 15
Antonelli, G.A.: AP+EL+MS+PS+SS+TF-TuA7, **14**
Avila, J.R.: TF+AP-TuM4, **11**
Avval, T.G.: TF+AP-TuM13, **13**
— B —
Bailey-Crandell, R.: 2D+AP+EM+MI+MN+NS+PS+TF-MoA5, 3
Balasubramanyam, S.: 2D+AP+EM+MI+NS+PS+TF-MoA5, **5**
Banerjee, P.: EM+2D+AP+NS+PS-TuM5, **9**
Basher, A.H.: AP+PS+TF-ThM5, **19**
Beckmann, K.: EM+2D+AP+NS+PS-TuM3, 9
belahcen, S.: AP+EL+MS+PS+SS+TF-TuA9, 14
Bignardi, L.: 2D+AP+EM+MI+MN+NS+PS+TF-MoA3, 3
Bilgilisoy, E.: AP+BI+PS+TF-WeM13, 17
Bol, A.A.: 2D+AP+EM+MI+NS+PS+TF-MoA5, 5
Bonvalot, M.: AP+EL+MS+PS+SS+TF-TuA9, 14
Bournel, F.: TF+2D+AP+EL+SS-MoA8, 7
Brann, M.R.: SS+2D+AP+AS+OX+SE-ThA1, 21
Brena, B.: TF+2D+AP+EL+SS-MoA8, 7
Bruner, P.: AP+EL+MS+PS+SS+TF-TuA9, 14
Bsiesy, A.: AP+EL+MS+PS+SS+TF-TuA9, 14
— C —
Cady, N.C.: EM+2D+AP+NS+PS-TuM3, **9**
Cai, H.: 2D+AP+EM+MI+NS+PS+TF-MoA3, 5
Canulescu, S.: 2D+AP+EM+MI+NS+PS+TF-MoA3, 5
Carver, V.: TF+AP-TuM13, 13
Cavanagh, A.S.: TF+AP-TuM5, 12
Chan, M.H.: AP-ThP1, 23
Chang, J.P.: AP+BI+PS+TF-WeM12, 17
Chang, Y.H.: TF+AP-TuM6, 12
Chaudhary, S.: TF+2D+AP+EL+SS-MoA8, 7
Chen, C.C.: AP-ThP1, 23
Chen, E.: AP+BI+PS+TF-WeM12, 17
Chen, F.Z.: AP-ThP1, 23
Chen, L.H.: AP+PS+TF-ThM4, **19**
Chen, W.-C.: AP-ThP1, 23
Cheng, P.: EM+2D+AP+NS+PS-TuM5, 9
Choi, C.: AP+BI+PS+TF-WeM12, 17
Chuang, H.-J.: 2D+AP+EM+MI+NS+PS+TF-MoA2, 5
Cobas, E.D.: 2D+AP+EM+MI+NS+PS+TF-MoA2, 5
— D —
D'Acunto, G.: TF+2D+AP+EL+SS-MoA8, 7
David, S.: AP+EL+MS+PS+SS+TF-TuA9, 14
Deng, X.: SS+2D+AP+AS+OX+SE-ThA10, **22**
Dickmann, M.: AP+BI+PS+TF-WeM1, 16
DiStasio, Jr., R.A.: AP+2D+EM+PS+TF-MoM9, 2
Duscher, G.: 2D+AP+EM+MI+NS+PS+TF-MoA3, 5
— E —
Eddy, C.R.: TF+2D+AP+EL+SS-MoA6, 7
Eddy, Jr., C.R.: TF+AP-TuM6, 12
Edel, R.: SS+2D+AP+AS+OX+SE-ThA2, **21**
Egger, W.: AP+BI+PS+TF-WeM1, 16
Elam, J.W.: AP+EL+MS+PS+SS+TF-TuA3, **14**
Emdadi, L.: 2D+AP+EM+MI+MN+NS+PS+TF-MoA8, **4**
Engstrom, J.R.: 2D+AP+EM+MI+NS+PS+TF-MoA11, **6**; AP+2D+EM+PS+TF-MoM9, 2
Eres, G.: 2D+AP+EM+MI+NS+PS+TF-MoA3, 5
Evans, J.W.: SS+2D+AP+AS+OX+SE-ThA6, 21
— F —
Fairbrother, D.: AP+BI+PS+TF-WeM13, 17
Feigelson, B.N.: 2D+AP+EM+MI+NS+PS+TF-MoA6, 5
Feygelson, B.: TF+2D+AP+EL+SS-MoA3, 7
Fink, K.: AP+PS+TF-ThM5, 19
Fischer, A.: AP+PS+TF-ThM3, **19**
Fujisaki, S.: AP+PS+TF-ThM1, 19
— G —
Gao, Z.: EM+2D+AP+NS+PS-TuM5, 9
Gassilloud, R.: AP+EL+MS+PS+SS+TF-TuA9, 14
Gasvoda, R.J.: AP+2D+EM+PS+TF-MoM2, **1**
Geohegan, D.: 2D+AP+EM+MI+NS+PS+TF-MoA3, **5**
George, A.: 2D+AP+EM+MI+NS+PS+TF-MoA9, 6
George, S.M.: AP+PS+TF-ThM10, 20; AP+PS+TF-ThM11, 20; AP+PS+TF-ThM6, 20; TF+AP-TuM12, 13; TF+AP-TuM5, 12
Georgiev, V.P.: EM+2D+AP+NS+PS-TuM13, **10**
Girolami, G.S.: TF+2D+AP+EL+SS-MoA5, 7
Goto, S.: EM+2D+AP+NS+PS-TuM6, 10
Grabnic, T.: SS+2D+AP+AS+OX+SE-ThA2, 21
Greenberg, B.: TF+2D+AP+EL+SS-MoA3, **7**
Grehl, T.: AP+EL+MS+PS+SS+TF-TuA9, 14
Grzeskowiak, J.: TF+AP-TuM6, 12
Gu, Y.: 2D+AP+EM+MI+NS+PS+TF-MoA3, 5
Gupta, G.: EM+2D+AP+NS+PS-TuM12, 10
— H —
Haastrup, M.J.: 2D+AP+EM+MI+MN+NS+PS+TF-MoA6, **4**
Hamada, I.: AP+PS+TF-ThM5, 19
Hamaguchi, S.: AP+BI+PS+TF-WeM3, 16; AP+BI+PS+TF-WeM4, 16; AP+PS+TF-ThM5, 19
Hanbicki, A.T.: 2D+AP+EM+MI+NS+PS+TF-MoA2, 5
Hausmann, D.M.: AP+2D+EM+PS+TF-MoM4, 1; AP+2D+EM+PS+TF-MoM8, 2
Hazra, J.H.: EM+2D+AP+NS+PS-TuM3, 9
Head, A.R.: TF+2D+AP+EL+SS-MoA8, 7
Hilfiker, J.N.: AP+EL+MS+PS+SS+TF-TuA1, **14**
Hodges, G.: TF+AP-TuM13, 13
Hsiao, C.N.: AP-ThP1, **23**
Hübner, U.: 2D+AP+EM+MI+NS+PS+TF-MoA9, 6
Hudson, E.A.: AP+2D+EM+PS+TF-MoM2, 1
Hugenschmidt, C.: AP+BI+PS+TF-WeM1, 16
— I —
Ideno, Y.: TF+AP-TuM11, 12
Inbar, H.S.: TF+AP-TuM6, 12
Ishibashi, S.: AP+BI+PS+TF-WeM1, 16
Isobe, M.: AP+BI+PS+TF-WeM4, 16; AP+PS+TF-ThM5, 19
Isshiki, H.: AP-ThP2, **23**
Ito, T.: AP+BI+PS+TF-WeM3, 16; AP+PS+TF-ThM5, 19
Izawa, M.: AP+PS+TF-ThM1, 19
— J —
Jaffal, M.: AP+EL+MS+PS+SS+TF-TuA9, 14
Jean-Jacques, J.-J.: TF+2D+AP+EL+SS-MoA8, 7
Johnson, N.S.: AP+PS+TF-ThM11, **20**
Johnson, S.D.: TF+2D+AP+EL+SS-MoA6, 7
Jones, J.: 2D+AP+EM+MI+NS+PS+TF-MoA10, 6
Jonker, B.T.: 2D+AP+EM+MI+NS+PS+TF-MoA2, 5
— K —
Kaiser, D.: 2D+AP+EM+MI+NS+PS+TF-MoA9, 6
Kalanyan, B.: TF+2D+AP+EL+SS-MoA10, 8
Karahashi, K.: AP+BI+PS+TF-WeM3, **16**; AP+BI+PS+TF-WeM4, 16; AP+PS+TF-ThM5, 19
Kato, T.: AP+PS+TF-ThM4, 19; TF+AP-TuM11, **12**
Kauffman, D.: SS+2D+AP+AS+OX+SE-ThA10, 22
Kawakami, R.: 2D+AP+EM+MI+MN+NS+PS+TF-MoA5, 3
Kawamura, K.: AP+PS+TF-ThM1, 19
Kelber, J.A.: 2D+AP+EM+MI+NS+PS+TF-MoA10, 6
Keller, N.: AP+EL+MS+PS+SS+TF-TuA7, 14
Kessels, W.M.M.: 2D+AP+EM+MI+NS+PS+TF-MoA5, 5; AP+2D+EM+PS+TF-MoM4, 1
Khoury, J.: AP+BI+PS+TF-WeM10, 17
Kim, J.: 2D+AP+EM+MI+MN+NS+PS+TF-MoA10, **4**
Knudsen, J.: TF+2D+AP+EL+SS-MoA8, 7
Kobayashi, H.: AP+PS+TF-ThM1, 19
Koschine, T.: AP+BI+PS+TF-WeM1, 16
Krstic, M.: AP+PS+TF-ThM5, 19
Kruse, N.: SS+2D+AP+AS+OX+SE-ThA7, 21
— L —
Lacovig, P.: 2D+AP+EM+MI+MN+NS+PS+TF-MoA3, 3
Lai, K.C.: SS+2D+AP+AS+OX+SE-ThA6, **21**
Lambeets, S.V.: SS+2D+AP+AS+OX+SE-ThA7, **21**
Lao, K.U.: AP+2D+EM+PS+TF-MoM9, 2
Larciprete, R.: 2D+AP+EM+MI+MN+NS+PS+TF-MoA3, **3**
Lauritsen, J.V.: 2D+AP+EM+MI+MN+NS+PS+TF-MoA6, 4
LaVoie, A.: 2D+AP+EM+MI+NS+PS+TF-MoA10, 6
Lee, I.: 2D+AP+EM+MI+MN+NS+PS+TF-MoA8, 4
Lee, Y.: AP+PS+TF-ThM11, 20
Lemaire, P.C.: AP+2D+EM+PS+TF-MoM8, 2
Liang, L.: 2D+AP+EM+MI+NS+PS+TF-MoA3, 5
Liehr, M.L.: EM+2D+AP+NS+PS-TuM3, 9
Lill, T.B.: AP+PS+TF-ThM3, 19
Lin, C.P.: AP-ThP1, 23
Lin, Y-C.: 2D+AP+EM+MI+NS+PS+TF-MoA3, 5
Linford, M.R.: TF+AP-TuM13, 13
Liu, C.: 2D+AP+EM+MI+NS+PS+TF-MoA3, 5
Liu, H.: TF+AP-TuM10, 12
Lizzit, D.: 2D+AP+EM+MI+MN+NS+PS+TF-MoA3, 3
Lizzit, S.: 2D+AP+EM+MI+MN+NS+PS+TF-MoA3, 3
Ludwig, K.F.: TF+2D+AP+EL+SS-MoA6, 7
Luo, G.: EM+2D+AP+NS+PS-TuM5, 9
Luo, YK.: 2D+AP+EM+MI+MN+NS+PS+TF-MoA5, **3**
Lyalin, I.: 2D+AP+EM+MI+MN+NS+PS+TF-MoA5, 3
— M —
Mackus, A.J.M.: 2D+AP+EM+MI+NS+PS+TF-MoA5, 5; AP+2D+EM+PS+TF-MoM4, **1**
Mahoney, L.: 2D+AP+EM+MI+MN+NS+PS+TF-MoA8, 4
Mahuli, N.: TF+AP-TuM12, **13**
Mameli, A.: AP+2D+EM+PS+TF-MoM3, 1

Author Index

Mammen, M.: 2D+AP+EM+MI+MN+NS+PS+TF-MoA6, 4
Martinazzo, R.: 2D+AP+EM+MI+MN+NS+PS+TF-MoA3, 3
Maslar, J.E.: TF+2D+AP+EL+SS-MoA10, 8
Matos-Abiague, A.: 2D+AP+EM+MI+MN+NS+PS+TF-MoA5, 3
Matsuda, S.: AP+BI+PS+TF-WeM13, 17
Matsukuma, M.: TF+AP-TuM11, 12
Matsuyama, H.: 2D+AP+EM+MI+MN+NS+PS+TF-MoA9, 4
McCreary, K.M.: 2D+AP+EM+MI+NS+PS+TF-MoA2, **5**
McElwee-White, L.: AP+BI+PS+TF-WeM13, 17; TF+AP-TuM1, **11**; TF+AP-TuM10, 12
McGhee, A.: EM+2D+AP+NS+PS-TuM13, 10
Melton, O.: AP+EL+MS+PS+SS+TF-TuA12, 15
Merkx, M.J.M.: 2D+AP+EM+MI+NS+PS+TF-MoA5, 5; AP+2D+EM+PS+TF-MoM4, 1
Mikkelsen, A.: EM+2D+AP+NS+PS-TuM10, **10**; TF+2D+AP+EL+SS-MoA8, 7
Mishra, M.: EM+2D+AP+NS+PS-TuM12, **10**
Mishra, R.: EM+2D+AP+NS+PS-TuM5, 9
Moran, A.J.: EM+2D+AP+NS+PS-TuM13, 10
Morikawa, Y.: AP+PS+TF-ThM5, 19
Mupparapu, R.: 2D+AP+EM+MI+NS+PS+TF-MoA9, 6
Murdzek, J.A.: AP+PS+TF-ThM6, **20**
— N —
Nabatame, T.: AP+BI+PS+TF-WeM1, 16
Naeemi, A.: EM+2D+AP+NS+PS-TuM1, **9**
Nakahata, K.: AP+PS+TF-ThM4, 19
Nakamura, H.: TF+AP-TuM11, 12
Nakamura, J.N.: 2D+AP+EM+MI+MN+NS+PS+TF-MoA9, **4**; EM+2D+AP+NS+PS-TuM6, 10
Nepal, N.: TF+2D+AP+EL+SS-MoA6, 7; TF+AP-TuM4, 11
Neumann, C.: 2D+AP+EM+MI+NS+PS+TF-MoA9, 6
Neupane, M.: 2D+AP+EM+MI+MN+NS+PS+TF-MoA5, 3
Newburger, M.: 2D+AP+EM+MI+MN+NS+PS+TF-MoA5, 3
Nguyen, V.: 2D+AP+EM+MI+MN+NS+PS+TF-MoA4, **3**
Ni, Z.: TF+AP-TuM11, 12
Nyakiti, L.O.: 2D+AP+EM+MI+NS+PS+TF-MoA6, 5
— O —
Ohtake, A.: EM+2D+AP+NS+PS-TuM6, 10
Opila, R.L.: AP+EL+MS+PS+SS+TF-TuA12, 15
Orlowski, M.K.: EM+2D+AP+NS+PS-TuM4, **9**
O'Toole, N.: AP+BI+PS+TF-WeM6, 17
— P —
Palmstrøm, C.J.: TF+AP-TuM6, 12
Parsons, G.N.: AP+2D+EM+PS+TF-MoM5, **1**
Pasquale, F.: 2D+AP+EM+MI+NS+PS+TF-MoA10, 6
Pelissier, B.: AP+EL+MS+PS+SS+TF-TuA9, 14
Pennachio, D.J.: TF+AP-TuM6, 12
Perea, D.E.: SS+2D+AP+AS+OX+SE-ThA7, 21
Pesce, V.: AP+EL+MS+PS+SS+TF-TuA9, 14
Phok, B.: AP+BI+PS+TF-WeM10, 17
Pilli, A.: 2D+AP+EM+MI+NS+PS+TF-MoA10, **6**
Poodt, P.: AP+2D+EM+PS+TF-MoM3, **1**
Posseme, N.: AP+EL+MS+PS+SS+TF-TuA9, 14
Potrepka, D.M.: AP+BI+PS+TF-WeM6, 17
Pribil, G.K.: AP+EL+MS+PS+SS+TF-TuA1, 14
Pulskamp, J.S.: AP+BI+PS+TF-WeM6, 17
Puretzky, A.A.: 2D+AP+EM+MI+NS+PS+TF-MoA3, 5
Puurunen, R.L.: AP+EL+MS+PS+SS+TF-TuA10, **14**
— R —
Rack, P.D.: 2D+AP+EM+MI+NS+PS+TF-MoA3, 5
Ramos, C.: TF+AP-TuM3, 11
Rayner, G.B.: AP+BI+PS+TF-WeM6, 17
Rehman, F.: TF+2D+AP+EL+SS-MoA8, 7
Robinson, Z.R.: TF+2D+AP+EL+SS-MoA6, 7; TF+AP-TuM6, 12
Rochet, F.: TF+2D+AP+EL+SS-MoA8, 7
Rodríguez-Fernández, J.: 2D+AP+EM+MI+MN+NS+PS+TF-MoA6, 4
Roozeboom, F.: AP+2D+EM+PS+TF-MoM3, 1
Rosenberg, S.G.: TF+2D+AP+EL+SS-MoA6, 7; TF+AP-TuM6, **12**
Rosenberger, M.R.: 2D+AP+EM+MI+NS+PS+TF-MoA2, 5
Rouleau, C.M.: 2D+AP+EM+MI+NS+PS+TF-MoA3, 5
Routzahn, A.: AP+PS+TF-ThM3, 19
— S —
Saare, H.: AP+2D+EM+PS+TF-MoM5, 1
Saisho, S.: AP-ThP2, 23
Salazar, B.G.: TF+AP-TuM10, **12**
Sánchez-de-Armas, R.: TF+2D+AP+EL+SS-MoA8, 7
Sandoval, T.E.: AP+2D+EM+PS+TF-MoM4, 1
Sang, X.: AP+BI+PS+TF-WeM12, **17**
Schnadt, J.: TF+2D+AP+EL+SS-MoA8, **7**
Serizawa, Y.: TF+AP-TuM11, 12
Setvin, M.: SS+2D+AP+AS+OX+SE-ThA8, **22**
Shamsi, Z.: TF+AP-TuM3, 11
Sharma, K.: AP+2D+EM+PS+TF-MoM8, 2
Shashkov, D.: AP+BI+PS+TF-WeM10, **17**
Shayesteh, P.: TF+2D+AP+EL+SS-MoA8, 7
Shinoda, K.: AP+PS+TF-ThM1, 19
Sibener, S.J.: SS+2D+AP+AS+OX+SE-ThA1, 21; SS+2D+AP+AS+OX+SE-ThA2, 21
Sobell, Z.: TF+AP-TuM5, **12**
Song, S.K.: AP+2D+EM+PS+TF-MoM5, 1
Sorescu, D.C.: SS+2D+AP+AS+OX+SE-ThA10, 22
Sperling, B.A.: TF+2D+AP+EL+SS-MoA10, **8**
Spiegelman, J.: TF+AP-TuM3, 11
Sridhara, K.: 2D+AP+EM+MI+NS+PS+TF-MoA6, **5**
Staude, I.: 2D+AP+EM+MI+NS+PS+TF-MoA9, 6
Strasser, A.: 2D+AP+EM+MI+NS+PS+TF-MoA3, 5
Strnad, N.A.: AP+BI+PS+TF-WeM6, **17**
Suga, T.: EM+2D+AP+NS+PS-TuM6, **10**
Suh, T.: 2D+AP+EM+MI+NS+PS+TF-MoA11, 6; AP+2D+EM+PS+TF-MoM9, **2**
Sumiya, M.: AP+BI+PS+TF-WeM1, 16
— T —
Takeya, K.: AP+PS+TF-ThM4, 19
Tanaka, Y.: AP-ThP2, 23
Tang, Z.: 2D+AP+EM+MI+NS+PS+TF-MoA9, 6
Taylor, H.: 2D+AP+EM+MI+MN+NS+PS+TF-MoA4, 3
Teplyakov, A.V.: AP+PS+TF-ThM12, **20**
Thind, A.: EM+2D+AP+NS+PS-TuM5, 9
Thompson, R.S.: SS+2D+AP+AS+OX+SE-ThA1, **21**
Thorman, R.: AP+BI+PS+TF-WeM13, **17**
Timm, R.: TF+2D+AP+EL+SS-MoA8, 7
Tinacba, E.J.C.: AP+BI+PS+TF-WeM4, **16**
Tortai, J-H.: AP+EL+MS+PS+SS+TF-TuA9, 14
Toyoda, N.: AP+BI+PS+TF-WeM5, **16**
Tran, D.: 2D+AP+EM+MI+MN+NS+PS+TF-MoA8, 4
Trioni, M.I.: 2D+AP+EM+MI+MN+NS+PS+TF-MoA3, 3
Troian, A.: TF+2D+AP+EL+SS-MoA8, 7
Tronic, T.: AP+BI+PS+TF-WeM12, 17
Tsyshevskiy, R.: TF+2D+AP+EL+SS-MoA8, 7
Turchanin, A.: 2D+AP+EM+MI+NS+PS+TF-MoA9, **6**
— U —
Uedono, A.: AP+BI+PS+TF-WeM1, **16**; AP+EL+MS+PS+SS+TF-TuA9, 14
Uematsu, K.: AP+BI+PS+TF-WeM5, 16
Urpelainen, S.: TF+2D+AP+EL+SS-MoA8, 7
Ushirozako, M.: 2D+AP+EM+MI+MN+NS+PS+TF-MoA9, 4
— V —
Vallee, C.: AP+EL+MS+PS+SS+TF-TuA9, **14**
van der Zande, A.M.: 2D+AP+EM+MI+MN+NS+PS+TF-MoA1, **3**
van Ommen, J.R.: TF+2D+AP+EL+SS-MoA1, **6**
VanDerslice, J.: AP+EL+MS+PS+SS+TF-TuA1, 14
Ventrice, Jr., C.A.: TF+AP-TuM6, 12
Visart de Bocarmé, T.: SS+2D+AP+AS+OX+SE-ThA7, 21
— W —
Walker, A.V.: TF+AP-TuM10, 12
Wallas, J.M.: TF+AP-TuM12, 13
Wang, K.: 2D+AP+EM+MI+NS+PS+TF-MoA3, 5
Wang, S.: AP+2D+EM+PS+TF-MoM2, 1
Wang, X.: TF+2D+AP+EL+SS-MoA11, **8**
Wang, Z.: AP+EL+MS+PS+SS+TF-TuA12, **15**
Wenzel, W.: AP+PS+TF-ThM5, 19
Wheeler, V.D.: TF+AP-TuM4, 11
Wiggins, B.: SS+2D+AP+AS+OX+SE-ThA2, 21
Winter, A.: 2D+AP+EM+MI+NS+PS+TF-MoA9, 6
Wollmershauser, J.A.: 2D+AP+EM+MI+NS+PS+TF-MoA6, 5; TF+2D+AP+EL+SS-MoA3, 7
Woodward, J.M.: TF+2D+AP+EL+SS-MoA6, **7**; TF+AP-TuM6, 12
— X —
Xiao, K.: 2D+AP+EM+MI+NS+PS+TF-MoA3, 5
Xu, W.: AP+2D+EM+PS+TF-MoM8, **2**
— Y —
Yalisove, R.: 2D+AP+EM+MI+NS+PS+TF-MoA11, 6
Yamaguchi, Y.: AP+PS+TF-ThM1, **19**
Yang, Y.: AP+2D+EM+PS+TF-MoM9, 2
Yngman, S.: TF+2D+AP+EL+SS-MoA8, 7
Yoon, M.: 2D+AP+EM+MI+NS+PS+TF-MoA3, 5
Young, E.C.: TF+AP-TuM6, 12
Yu, Y.: 2D+AP+EM+MI+NS+PS+TF-MoA3, 5
Yuan, B.: AP+EL+MS+PS+SS+TF-TuA12, 15
— Z —
Zhang, W.: 2D+AP+EM+MI+NS+PS+TF-MoA3, 5
Zhang, Z.: AP+2D+EM+PS+TF-MoM2, 1; TF+2D+AP+EL+SS-MoA5, **7**
Zhou, T.: 2D+AP+EM+MI+MN+NS+PS+TF-MoA5, 3
Zutic, I.: 2D+AP+EM+MI+MN+NS+PS+TF-MoA5, 3